A Sr, Nd, and Pb isotopic study of mantle domains and crustal structure from Miocene volcanic rocks in the Mojave Desert, California

Jonathan S. Miller* } *Department of Geology, University of North Carolina,*
Allen F. Glazner } *Chapel Hill, North Carolina 27599-3315, USA*

G. Lang Farmer *CIRES and Department of Geological Sciences, University of Colorado, Boulder, Colorado 80309, USA*

Ismail B. Suayah } *Department of Geology, University of North Carolina,*
Lori A. Keith } *Chapel Hill, North Carolina 27599-3315, USA*

ABSTRACT

Tertiary volcanic rocks were erupted across the Mojave Desert and southeastern California in the early to middle Miocene after a long period of magmatic quiescence. Eruption of these rocks generally coincided with regional extension. New Sr, Nd, and whole-rock Pb isotopic data for Miocene rocks, from a transect from the western Mojave Desert to the Colorado River trough, provide clues to crustal and mantle structure during this important time period. Volcanism was calc-alkalic but transitional to alkalic in the eastern part of the area. Trace element contents, trace element ratios, and radiogenic isotopic compositions vary across the study area, and isotopic composition is correlated with both bulk chemical composition and longitude. Correlation of isotopic composition with bulk composition results from widespread contamination of mantle-derived basalts with crust. Variation of isotopic composition versus longitude for rocks of all bulk compositions reflects longitudinal variations in both mantle and crustal structure. Geochemical signatures of mafic rocks east of about long 116°W indicate an ancient (Precambrian) enriched lithosphere source. Some thinned and/or reworked Precambrian crust extends west of 116°W. Mafic rocks west of 116°W were derived from mantle with oceanic geochemical and isotopic signatures. There is no clear, coincident, major crustal structure or tectonic boundary in surface geology at 116°W; however, modern-day seismicity is restricted to areas west of this longitude, and there is a change in the dominant orientation of mountain ranges at this longitude. The data here also indicate that the long-standing problem of drawing the $Sr_i = 0.706$ line through the Mojave Desert can be resolved if the line represents the west edge of the North American mantle rather than Precambrian crust. By this definition, the $Sr_i = 0.706$ line would be the isotopic boundary at 116°W. The cause of early Miocene volcanism in the Mojave Desert remains enigmatic. An oceanic mantle source for early Miocene basalts in the western Mojave Desert suggests a possible connection to asthenospheric mantle volcanism in the California Coast Ranges. Simple models of decompression melting of enriched mantle following convective thinning and extension of the lithosphere cannot be applied across the Mojave Desert.

Keywords: extension tectonics, isotopes, magma contamination, miocene, Mojave Desert, Precambrian, Rand Schist.

INTRODUCTION

Geochemical and isotopic studies of volcanic rocks from the western United States have been important in shaping modern views of lithospheric structure of the North American Cordillera and in developing models for continental extension and extension-related magmatism (e.g., Perry et al., 1987; Menzies, 1989; Gans et al., 1989; Fitton et al., 1991; Walker and Coleman, 1991; Livaccari and Perry, 1993; Asmerom et al., 1994; Hawkesworth et al., 1995; Rogers et al., 1995; Beard and Johnson, 1997). These studies have focused on (1) using regional variability in the isotopic signatures of volcanic rocks in the Basin and Range to map spatially variable lithospheric structure and (2) the temporal shifts in magma-source compositions and their relationships to tectonic history and timing and mode of lithospheric extension.

Except for a few studies in the extended areas of southern Nevada, western Arizona, and southeasternmost California (e.g., Farmer et al., 1989; Feuerbach et al., 1993; Bradshaw et al., 1993), the Mojave Desert region has been a significant gap in an otherwise large body of geochemical and isotopic work on synextensional magmatism in the U.S. Cordillera. The Mojave Desert and southeastern California–western Arizona are of special interest because they link the stable plate-interior areas of the Colorado Plateau to the dynamic plate boundary and because early Miocene volcanism was synchronous from the plate boundary to the Colorado Plateau (Glazner and Supplee, 1982). The causes of volcanism across the region may thus be related as much to kinematic and thermal effects of plate subduction at the evolving plate boundary as to gravitationally induced extension and decompression melting of the mantle, which has been frequently invoked in some of the studies already mentioned to explain mid-Tertiary volcanism in other parts of the U.S. Cordillera.

This study contains a considerable amount of new whole-rock Sr, Nd, and Pb isotopic data but also partly complements an earlier regional Sr and O isotopic study of Glazner and O'Neil (1989) that left important questions regarding lithospheric structure unresolved. Glazner and O'Neil (1989) showed that regular variations in isotopic composition occurred from east to west across the Mojave Desert, but it was unclear whether these isotopic variations corresponded to abrupt or gradual changes in mantle and crustal domains and whether they correlated coherently with surface geology.

*Present address: Department of Geology, San Jose State University, San Jose, California 95192-0102, USA; e-mail: jsmiller@email.unc.edu.

GSA Bulletin; August 2000; v. 112; no. 8; p. 1264–1279; 12 figures; 1 table.

We use geochemical and isotopic data from synextensional Miocene volcanic rocks erupted across the Mojave Desert and southeastern California to reexamine lithospheric structure in light of surface geology and tectonic history. A considerable amount of geochemical and isotopic data related to the evolution of the Proterozoic crust and Mesozoic arc in the Mojave Desert has also been published since the decade-old study of Glazner and O'Neil (1989), and some of this work bears directly on our discussion (Wooden and Miller, 1990; Young et al., 1992; Miller and Wooden, 1994; Miller and Glazner, 1995; Miller et al., 1995).

From a regional perspective, our data show a considerable amount of chemical and isotopic variability as in the Glazner and O'Neil (1989) study. The variability in chemical and especially isotopic composition must reflect varying mantle sources, the amount of crustal contamination and the kind of recycled crust, and possibly the degree of partial melting of the different mantle sources. Sorting out these competing petrologic factors is difficult, especially the issue of crustal contamination. Crustal contamination is nearly ubiquitous in Miocene rocks erupted throughout the Mojave Desert and southeastern California and presents a formidable problem for investigating mantle-source variations (Glazner, 1990; Miller and Miller, 1991; Miller et al., 1998). Basalts erupted during the early Miocene, and before or during peak extension, are rare in many areas. We emphasize at the outset that it is difficult to quantify satisfactorily the degree to which even the most mafic rocks in the data set have been crustally contaminated. Our approach considers rocks that span the compositional range in different areas, and these data arrays are used to extrapolate probable mantle sources. Our regional data set and some simple geochemical arguments indicate that the variation in isotopic and geochemical reservoirs is quite appreciable across the Mojave Desert and southeastern California, and these variations must reflect major heterogeneities in the mantle and crust across the area.

REGIONAL GEOLOGY

Tertiary Volcanic Fields

Tertiary volcanic rocks in this study come from a fairly restricted latitude, between about 34.5°N and 35.5°N (Fig. 1). Volcanism commenced within this latitude at ca. 22 Ma and had ceased by ca. 18 Ma (cf. Glazner and Supplee, 1982; Howard and John, 1987; Sherrod and Nielson, 1993; Miller et al., 1998). In many of the volcanic sections from which the samples in this study were taken, the 18.5 Ma Peach Springs Tuff (Nielson et al., 1990; Miller et al., 1998) is the uppermost volcanic rock in the stratigraphy. A few samples from the Fort Irwin area are slightly younger (ca. 16 Ma; E. L. Schermer, 1994, written commun.). All of the rocks in this study have early to middle Miocene ages that generally coincide with regional extension, although regional extension did not affect all areas to the same degree (Howard and John, 1987; Glazner et al., 1989; Nielson and Beratan, 1990; Walker et al., 1995; Nielson and Beratan, 1995; Miller et al., 1998).

In many of the middle Tertiary sections where extension is evident, and volcanic centers were nearby, volcanic rocks are among the earliest strata preserved or are intercalated with early syntectonic sedimentary rocks (cf. Nielson and Beratan, 1990; Hileman et al., 1990; Sherrod and Nielson, 1993; Fillmore et al., 1994; Nielson and Beratan, 1995; Miller et al., 1998). Thus volcanism either preceded or occurred right at the onset of extension. Most of the volcanic fields consist of cinder cones and associated flows, composite domes and plug flows, and some andesite stratocones (Hazlett, 1986; Glazner, 1988; Miller, 1989; Sabin et al., 1994). All of the volcanic fields in the study area erupted calc-alkalic rocks with a predominance of intermediate composition rocks (andesites and dacites) over either basalts or rhyolites (Hazlett, 1986; Glazner, 1988; Glazner, 1990; Miller and Miller, 1991; Suayah et al., 1992; Keith et al., 1994; Sabin et al., 1994).

Pre-Tertiary Rocks

Across the region there are major differences in the pre-Tertiary geology (Fig. 1). Precambrian basement and cratonal passive-margin strata are widespread in the eastern half of the study area (from the Bristol Mountains to the Colorado River trough; Fig. 1; Stone et al., 1983; Wooden and Miller, 1990). In the central Mojave Desert, rare outcrops of Precambrian basement and scattered but abundant outcrops of transitional cratonal and miogeoclinal rocks are inferred to define an approximate craton margin (Martin and Walker, 1992; Fig. 1). Paleozoic eugeoclinal rocks are found north and west of Barstow (Carr et al., 1992; Fig. 1). In the western Mojave Desert, metagraywacke and metabasaltic basement rocks (Pelona-Orocopia-Rand schists) are exposed in the Rand Mountains and at Portal Ridge (Jacobson et al., 1988; Fig. 1). Thus, crudely from east to west there is a transition from autochthonous cratonic basement to allochthonous oceanic basement of varying age. Whether this transition is abrupt or gradual is not clear on the basis of the exposed geology, in part because the entire area was intruded by Mesozoic plutons that reworked much of the pre-Mesozoic crust (Miller and Wooden, 1994; Miller and Glazner, 1995). Although no known Precambrian crust is exposed in surface geology along the transect west of the Barstow area, it could possibly be present in the deeper crust, and some zircon geochronologic data implies that Precambrian crust may have been present as far west as Barstow (Fig. 1) Miocene (Walker et al., 1995).

GEOCHEMICAL AND ISOTOPIC DATA

Discussion of the analytical methods used in obtaining these data can be found in Miller and Glazner (1995) and in the footnote to Table 1. Some of the geochemical and isotopic data have been published elsewhere (Glazner and O'Neil, 1989; Glazner, 1990; Miller and Miller, 1991). The reader is referred to these publications for much of the additional data not presented in Table 1. A complete database containing all data for these rocks is available from the first author. In order to discuss the geochemical and isotopic variability in these rocks, we break the data into three groups based on silica content. Rocks with <55 wt% SiO_2 are considered mafic. Rocks having 55 to 65 wt% SiO_2 are considered intermediate-composition rocks, and silicic rocks have >65 wt% SiO_2. We also make an arbitrary division of the transect into three sectors at meridians of longitude as in the earlier study of Glazner and O'Neil (1989). As it turns out, one of these longitudinal breaks corresponds with a fairly significant change in lithospheric structure.

Major Elements

The major element compositions of the rocks are broadly similar across the study area and are calc-alkalic. Although Mafic rocks have a range of Al_2O_3 and TiO_2 contents, this variation probably reflects more than one parental basalt type (Table 1) and/or variable amounts of fractionation. There is no apparent longitudinal variation in either Al_2O_3 or TiO_2. The mafic rocks do show a scattered but generally increasing total alkali abundance from west to east (Fig. 2A); most of this variation is due to increasing K_2O (Fig. 2B). Although the data scatter to lower values, rocks having >2.0 wt% K_2O are restricted to areas east of ~116°W. Thus mafic rocks in the eastern part of the study area are alkalic. No distinct major element variation is apparent for rocks with higher silica contents.

Trace Elements

Regional variation is also evident among several key trace elements and elemental ratios. For mafic rocks, the concentrations of Sr, Ba, and Nd increase in abundance from west to east (Fig. 3).

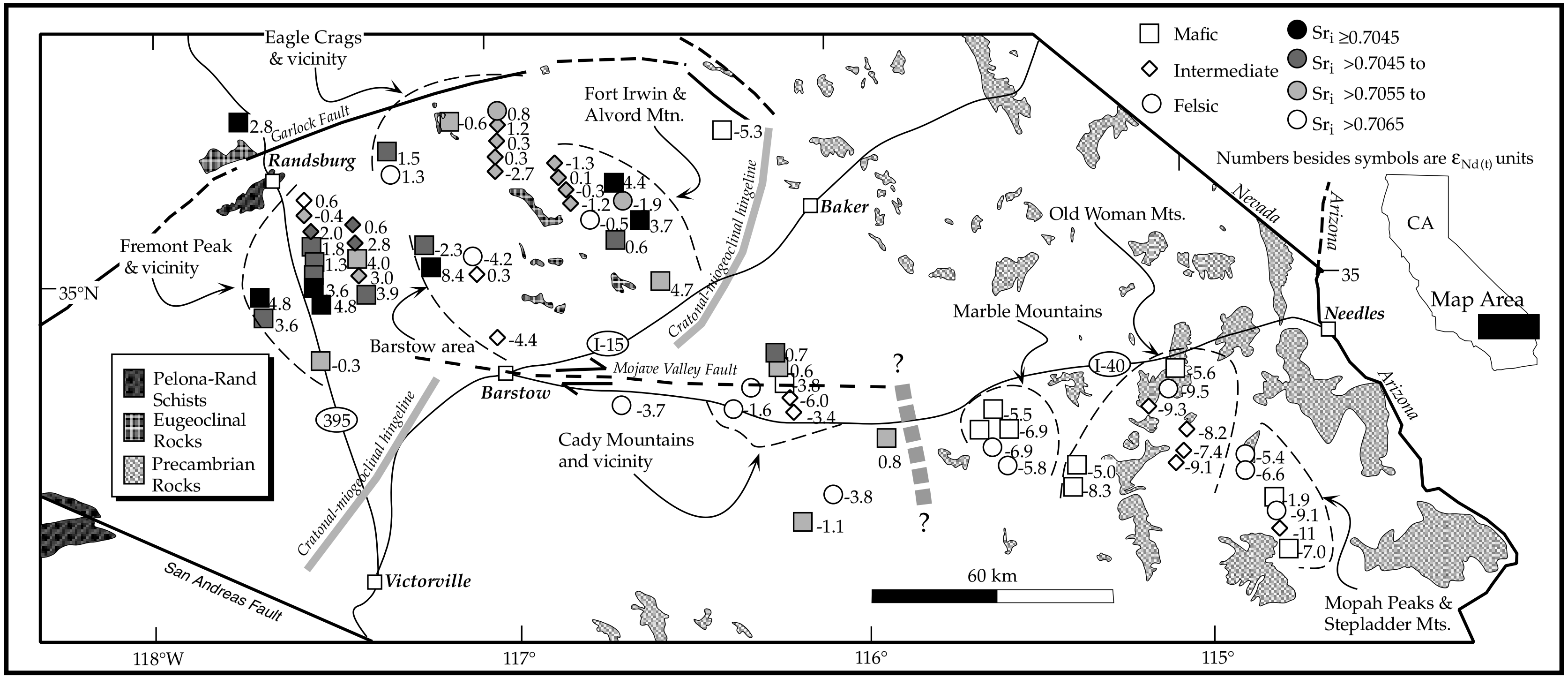

Figure 1. Map showing approximate locations, ranges of Sr_i and $\varepsilon_{Nd(t)}$ of data samples, and relationship to important paleogeographic and tectonic elements of the Mojave Desert. Samples from the southern Black Mountains, near the Nevada-Arizona state boundary (see Table 1), are not shown. Precambrian basement rocks are abundant in the eastern Mojave Desert, and oceanic rocks are abundant in the western Mojave Desert. Mesozoic intrusive rocks are not shown. Cratonal-miogeoclinal hinge line is from Martin and Walker (1992), and Mojave Valley fault is from Martin et al. (1993). Isotopic composition is broadly correlated with surface geology. Especially important are the differences in basalt isotopic values to the east and west of heavy shaded-dash line, which approximately marks the isotopic break at 116°W. Precambrian crust extends farther west than this boundary as inferred from Sr_i and $\varepsilon_{Nd(t)}$ values of intermediate-composition to felsic rocks, but ancient enriched-mantle lithosphere is absent west of this boundary. Eastern extension of the Mojave Valley fault is uncertain (see Martin et al., 1993). Lithosphere variations significantly south and west of Barstow are less certain owing to fewer exposures of Tertiary volcanic rocks.

Between about 116° and 115.5°W, Sr contents are, with one exception, less than 600 ppm, but east of this longitude, they approach 1200 ppm (Fig. 3A). Nd takes an even more distinct jump in concentration marked by an inflection in the longitudinal trend (Fig. 3B); west of 116°W, Nd concentration is uniformly <30 ppm whereas Nd concentrations approach 100 ppm east of 116°W (Fig. 3B). The trend for Ba in the mafic rocks has a similar but less well developed inflection again at about 116°W (Fig. 3C). Ratios of high field strength elements (HFSEs) to incompatible elements are scattered for the mafic rocks, but Zr/Ba ratios are uniformly low east of about 116°W (Fig. 4A). All mafic rocks are enriched in light rare earth elements (LREEs) relative to chondrites (Table 1), but the mafic rocks in the eastern part of the study area are enriched to a greater degree as shown by their higher La/Yb_N ratios (Fig. 4B).

Representative samples of eastern and central Mojave basalts highlight the geochemical distinctions on an element normalization diagram (Fig. 5). Sample SV-2 from the Old Woman Mountains area and sample ALVO-3 (Table 1) from Alvord Mountain are both true basalts (<49 wt% SiO_2; >7 wt% MgO; >100 ppm Ni, >250 ppm Cr; P_2O_5/K_2O >0.3; see subsequent discussion) with phenocrystic olivine and no petrographic evidence of contamination (i.e., no spongy plagioclase or quartz xenocrysts). ALVO-3 is separated by about a degree of longitude from SV-2 and illustrates the transition in trace element chemistry from west to east across ~116°W longitude. Both basalts show an overall enrichment in large ion lithophile elements (LILEs) and LREEs relative to N-MORB (normal mid-oceanic-ridge basalt), but the enrichment of highly incompatible elements is 10 times greater in SV-2, which is also enriched in the middle and heavy REEs. SV-2 also has a modest depletion in Nb relative to the LILEs and LREEs, whereas ALVO-3 has no comparable depletion.

Intermediate-composition to silicic rocks (>55 wt% SiO_2) do not exhibit trace element versus longitude trends that are as coherent as those for the mafic rocks. Rb and Sr are scattered when plotted versus longitude. Ba and Nd increase eastward for intermediate-composition and silicic rocks, and Ba shows the same inflection as seen in the mafic rocks (Table 1), but no observable trend is seen for Zr/Ba ratios for the intermediate-composition and silicic rocks (Fig. 4A). As with the mafic rocks, intermediate-composition and silicic rocks generally have greater LREE enrichment relative to chondrites moving to the east (Fig. 4B).

Sr, Nd, and Pb Isotopes

Sr and Nd initial isotopic ratios correlate with bulk composition and geographic position (Figs. 6–9). Glazner and O'Neil (1989) found that Sr_i increases and $\delta^{18}O$ decreases eastward from the Mojave Desert into southeastern California. Figures 6 and 7 verify this scattered, roughly linear, correlation of Sr_i with longitude and SiO_2. Not surprisingly, the new data from this study show that $\varepsilon_{Nd(t)}$ is also correlated with longitude and SiO_2 content (Figs. 8 and 9). Generally, the intermediate-composition and silicic rocks show somewhat less scatter in both Sr_i and $\varepsilon_{Nd(t)}$ versus longitude (Figs. 6 and 8) compared to the mafic rocks. At any given longitude, the mafic rocks generally extend to lower Sr_i and higher $\varepsilon_{Nd(t)}$ than any of the intermediate-composition or silicic rocks (see limiting lines in Figs. 6 and 8).

Pb isotopic ratios are not as well correlated with bulk composition and longitude as Sr_i and $\varepsilon_{Nd(t)}$. Pb isotopic ratios generally do not show as high a degree of correlation as Sr_i and $\varepsilon_{Nd(t)}$ with bulk composition, but $^{206}Pb/^{204}Pb$ is weakly correlated with SiO_2 (Table 1). Generally, $^{206}Pb/^{204}Pb$ values for mafic rocks and for intermediate-composition and silicic rocks decrease to the east and become more scattered (Fig. 10A). In contrast to the Sr and Nd data, mafic rocks and intermediate-composition and silicic rocks show complete overlap in Pb isotopic composition. Nearly all $^{206}Pb/^{204}Pb$ values west of 116°W for mafic, intermediate-composition, and silicic rocks are greater than 19.0 (Fig. 10A). $^{208}Pb/^{204}Pb$ increases slightly from west to east for mafic rocks and for intermediate-composition and silicic rocks, but the trend is not as well defined as the $^{206}Pb/^{204}Pb$ trend (Fig. 10B)

DISCUSSION

The data reported in this study bear on a number of important issues regarding the Tertiary and pre-Tertiary geologic evolution of the southern Basin and Range. We address in subsequent sections several of these in the context of this study and recent previous work in the Mojave Desert. These include (1) the nature of the subcontinental mantle across the Mojave Desert, (2) variations in crustal structure across the Mojave Desert, (3) the problem of the Sr_i = 0.706 line, and (4) the probable causes and triggering mechanisms for volcanism.

Mantle Domains to the West and East of 116°W

An important part of this study is identification of the parental basalts in terms of their trace element and isotopic composition. The parental basalts not only provide important end members for mixing models but also give clues to the nature, structure, and tectonic history of the mantle beneath the Mojave.

Inferring mantle sources in these rocks is a formidable problem. The complete overlap in the Pb data between mafic, intermediate-composition, and silicic rocks indicates that many of the mafic rocks have been contaminated with crust. The low Pb concentrations of most basalts makes them highly sensitive to even small amounts of crustal contamination. However, because the mafic rocks extend to lower Sr_i and higher $\varepsilon_{Nd(t)}$ values than any of the intermediate-composition and silicic rocks (at any given longitude), it is possible to place limits on the mantle Sr and Nd isotopic signature. Because crustal contamination is the overriding cause of Sr and Nd isotopic correlation with bulk composition, the data can potentially be used to extrapolate back to the Sr_i and $\varepsilon_{Nd(t)}$ of subcrustal mantle sources in the different areas. The limit lines shown in Figures 6 and 8 give a crude approximation to the longitudinal variation in probable mantle sources in terms of Sr and Nd isotopic composition. The data are scattered but at first glance suggest a continuous transition from west to east. Vertical deviations away from these limit lines are due to crustal contamination.

Glazner and O'Neil (1989) examined the correlation among isotopic ratio, longitudinal position, and crustal contamination by fitting their data to a plane of the form $x = a + by + cz$, where x is the Sr_i value, y is SiO_2 contents (in wt%), z is longitude in positive degrees, and a, b, and c are fitting coeficients. The Sr_i data in this study can also be fitted to a plane and give results similar to those of Glazner and O'Neil (1989), i.e., Sr_i increases by 0.0015 for each degree of eastward longitude and by 0.0001 for each 1 wt% increase in SiO_2. Treating $\varepsilon_{Nd(t)}$ as the dependent variable also gives a statistically reasonable planar fit. However, the planar fits tend to smooth the data. Fitting only the mafic rock isotopic data produces a poorer fit, and trace element variations (Figs. 3 and 4) indicate that the gradual isotopic shift implied by the fitting planes (and the limit lines in Figs. 6 and 8) does not accurately reflect changes in lithospheric structure from west to east.

West of 116°W. Extrapolating the contamination vectors by eye (Figs. 7 and 9) suggests that mafic rocks from the western Mojave (~117°W) were derived from mantle with a minimum Sr_i of ~0.703–0.704) and maximum $\varepsilon_{Nd(t)}$ of about +8. Scatter in the data permits somewhat higher Sr_i and lower $\varepsilon_{Nd(t)}$ components as well. Rocks between 117°W and 116°W define a contamination trend that extrapolates back to a mantle source similar to rocks from west of 117°W. The low Sr_i and high $\varepsilon_{Nd(t)}$ values are similar to MORB-type values reported in early Miocene basalts from the California Coast Ranges, west of the Mojave Desert (e.g., Johnson and O'Neil, 1984; Cole and

TABLE 1. ANALYTICAL DATA FOR MIOCENE VOLCANIC ROCKS FROM THE MOJAVE DESERT

Sample	General locale	Long (W)	Rb	Sr	$\frac{^{87}Sr}{^{86}Sr}$	Sr_i	Sm	Nd	$\frac{^{143}Nd}{^{144}Nd}$	$\varepsilon_{Nd(t)}$	$\frac{^{206}Pb}{^{204}Pb}$	$\frac{^{207}Pb}{^{204}Pb}$	$\frac{^{208}Pb}{^{204}Pb}$	SiO_2	TiO_2	Al_2O_3	Na_2O	K_2O	P_2O_5	Ba	Zr/Ba	$\frac{La}{Yb}_{(N)}$
CS-W/PST	S. Black Mountains	114.22°					1.850	41.99	0.512046	–11	18.23	15.59	39.12									
CS-B/PST	S. Black Mountains	114.22°	212	41.10	0.71515	0.7112	7.220	42.02	0.512030	–12												
CS-G/PST	S. Black Mountains	114.22°	215	42.30	0.71560	0.7117	7.543	24.73	0.512019	–12	18.23	15.59	39.11									
A-2	Mopah Range	114.75°	54.0	815.2	0.70883	0.7088	9.319	54.57	0.512270	–7				53.5	1.38	16.30	3.25	2.58	0.49			
A3-1	Mopah Range	114.76°	26.7	1049	0.70762	0.7076	17.65	100.2	0.512531	–2				44.5	1.59	13.00	2.50	2.00	0.93			
1215-1	Mopah Range	114.76°	76.7	610.5	0.70940	0.7093	5.622	35.35	0.512039	–11				63.0	0.54	14.90	3.39	3.47	0.21	1390	0.13	
19-1	Mopah Range	114.77°									18.40	15.55	39.02	64.4	0.70	16.00	3.68	4.28	0.21	1300	0.30	
A-14	Mopah Range	114.78°	109	409.8	0.71021	0.7100	4.039	25.59	0.512163	–9	18.42	15.56	39.01	68.2	0.40	14.80	3.51	0.40	0.10			
PCST-37	Stepladder Mountains	114.86°	103	375.0	0.70832	0.7081	9.830	59.03	0.512349	–5	18.94	15.66	39.11	71.0	0.51	14.19	4.28	4.48	0.15	1300	0.33	19.33
ST-HA-2	Stepladder Mountains	114.86°	59.1	867.7	0.70803	0.7080	4.813	27.07	0.512287	–7	19.01	15.66	39.07	66.0	0.81	16.84	4.00	2.66	0.24	930	0.16	17.81
LP-KB	Old Woman Mountains	115.07°	62.0	846.0	0.70904	0.7090	6.740	40.95	0.512206	–8	18.71	15.66	39.28	59.3	1.08	17.47	3.93	2.80	0.36	1100		22.75
PLB	Old Woman Mountains	115.07°	51.0	1180	0.70838	0.7084	12.49	75.91	0.512337	–6	18.86	15.65	39.05	53.8	1.18	14.30	3.05	2.60	0.60	1300	0.16	32.32
LP-UB3	Old Woman Mountains	115.07°	68.0	443.0	0.70873	0.7086	3.770	21.63	0.512248	–7	18.80	15.69	39.37	61.1	0.68	14.95	3.10	2.80	0.16	979		29.72
T-ub	Old Woman Mountains	115.11°	42.7	674.5	0.71031	0.7103	6.272	35.63	0.512158	–9				57.5	1.10	17.31	3.15	1.75	0.28	1052		18.24
P2-C	Old Woman Mountains	115.14°	171	530.0	0.71043	0.7102	9.770	66.53	0.512135	–10	18.48	15.66	39.22	66.1	0.80	16.71	3.66	5.08	0.13	1600	0.28	32.67
EP-1	Old Woman Mountains	115.15°	48.0	1434	0.70963	0.7096	10.70	67.21	0.512148	–9	18.48	15.63	39.20	56.2	1.08	17.51	4.06	2.75	0.43	1641		34.84
SV-2	Old Woman Mountains	115.37°	45.0	1134	0.70768	0.7077	15.01	89.01	0.512372	–5	18.98	15.65	39.05	48.6	1.56	16.13	2.47	2.29	1.03	1837	0.14	33.04
SV-3	Old Woman Mountains	115.37°	39.0	1111	0.70877	0.7087	10.15	66.13	0.512200	–8	18.79	15.66	39.24	54.3	1.22	16.97	3.72	2.56	0.63	1200		32.80
MARB-22	Marble Mountains	115.64°	44.0	513.0	0.70816	0.7081	4.723	23.72	0.512286	–7				53.0	1.18	17.10	3.38	1.21	0.26	529	0.31	
MARB-23	Marble Mountains	115.64°	44.0	704.1	0.70794	0.7079	7.785	43.97	0.512343	–6				52.7	1.20	16.20	3.28	1.91	0.34	687	0.26	
MARB-2	Marble Mountains	115.64°	327	464.0	0.70904	0.7085	5.159	33.97	0.512273	–7	18.60	15.61	39.22	71.9	0.37	15.30	3.89	3.63	0.07	952	0.20	20.84
MARB-9	Marble Mountains	115.64°	34.0	521.0		0.7080								53.1	1.14	16.80	3.25	1.52	0.25	548	0.27	
MARB-24	Marble Mountains	115.65°	97.0	406.0	0.70809	0.7079	4.282	28.16	0.512325	–6	18.71	15.60	39.05	73.6	0.36	13.50	3.90	3.94	0.10	925	0.19	
M84LH108	Lava Hills	115.94°	39.6	650.8	0.70626	0.7062	4.775	23.08	0.512672	1				54.7	1.45	16.30	3.61	1.63	0.30			
LVHL-2	Lava Hills	115.96°	73.9	726.7	0.70789	0.7078	3.653	19.12	0.512432	–4	19.11	15.61	38.91	65.8	0.71	16.20	4.27	2.65	0.14	898	0.18	
NBPS-6	Bullion Mountains	116.15°	28.0	544.0	0.70583	0.7058	6.045	21.72	0.512577	–1				48.9	1.88	16.70	3.53	1.16	0.43	374	0.52	5.49
22-10A	Cady Mountains	116.24°	101	597.0	0.70814	0.7080	4.507	24.73	0.512449	–3	19.11	15.66	39.18	64.3	0.94	16.50	4.28	2.98	0.21	956	0.19	
AG-2	Cady Mountains	116.24°	110	448.0	0.70866	0.7085	4.760	29.44	0.512315	–6	18.76	15.68	39.33	63.2	0.76	16.40	5.01	3.20	0.33	981	0.35	13.15
13-22	Cady Mountains	116.24°	54.0	523.0	0.70589	0.7058	6.040	28.54	0.512658	1	19.19	15.68	39.20	53.1	2.25	16.20	3.83	2.09	0.50	583	0.37	
12–3	Cady Mountains	116.24°	32.0	553.0	0.70565	0.7055	7.537	27.46	0.512676	1				50.0	2.65	16.20	3.69	1.54	0.55	500	0.40	6.91
11-90	Cady Mountains	116.28°	35.0	876.0	0.70733	0.7073	4.940	22.40	0.512434	–4	18.99	15.69	39.18	52.7	2.13	19.20	4.09	1.77	0.22	748	0.21	
25-13	Cady Mountains	116.30°	116	554.0	0.70723	0.7071					19.07	15.64	38.50	68.8	0.44	16.10	4.18	3.64	0.09	808	0.19	
82-25	Cady Mountains	116.32°	121	683.0	0.70702	0.7069	4.030	22.37	0.512543	–2	19.07	15.62	38.94	68.3	0.40	15.60	4.09	4.09	0.14	901	0.20	
a-3*	Avawatz Mountains	116.49°	42.0	1289	0.70742	0.7074	8.801	50.49	0.512358	–5	19.11	15.65	39.00	53.4	1.06	15.04	3.52	2.34	0.27	1684	0.07	
ALVO-3	Alvord Mountain	116.55°	18	473.0	0.70603	0.7060	4.150	16.90	0.512854	5				48.7	1.63	17.10	2.78	0.91	0.52	194	0.63	5.49
A4-2	Newberry Mountains	116.67°	191	767.6	0.70788	0.7077	4.127	22.88	0.512438	–4				69.1	0.50	15.80	3.96	1.80	0.13	782	0.24	
89fi6*	Fort Irwin	116.68°	6.0	291.4	0.70448	0.7045	3.059	10.59	0.512828	4	19.28	15.68	39.06	48.2	1.26	16.89	3.20	0.33	0.33	136	1.17	
91fi102*	Fort Irwin	116.69°	42.0	715.6	0.70582	0.7058	3.391	18.22	0.512531	–2	19.14	15.67	38.94	65.7	0.62	17.16	4.27	2.22	0.21	833	0.25	
93fi12*	Fort Irwin	116.75°	7.0	309.4	0.70420	0.7042	3.027	10.23	0.512860	4				49.1	1.24	17.84	3.24	0.29	0.21	148	0.97	
91fi5*	Fort Irwin	116.79°	16.0	538.1	0.70548	0.7055	3.959	17.43	0.512661	1	19.16	15.65	39.00	51.5	1.18	18.13	3.57	0.84	0.36	367	0.55	
90fi39*	Fort Irwin	116.80°	140	32.8	0.71005	0.7075	4.703	19.49	0.512606	–1	19.29	15.69	39.13	75.6	0.09	14.32	3.46	5.67	0.02	409	0.35	
90fi38*	Fort Irwin	116.81°	47	557.4	0.70598	0.7059	4.356	23.70	0.512567	–1	19.24	15.67	39.01	63.3	0.62	16.86	4.78	2.54	0.28	882	0.28	
90fi28*	Fort Irwin	116.86°	74	421.3	0.70624	0.7061	4.894	24.49	0.512614	0	19.20	15.67	39.05	64.0	0.69	16.72	3.90	3.58	0.20	905	0.32	
91fi9p*	Fort Irwin	116.87°	28	702.3	0.70526	0.7052	5.013	24.81	0.512634	0	19.08	15.64	38.87	55.1	1.21	16.83	4.41	1.60	0.37	512	0.27	
91fi12p*	Fort Irwin	116.87°	40	686.8	0.70576	0.7057	4.905	24.68	0.512563	–1	19.13	15.64	38.90	56.0	1.01	16.30	4.16	1.76	0.32	579	0.37	
BARS-2	Barstow	116.89°	80.6	559.9	0.70694	0.7068	4.249	22.35	0.512402	–4	19.24	15.64	38.84	70.0	0.41	15.80	4.00	3.36	0.11	830	0.20	11.95
LNMT-2	Lane Mountain	116.94°									19.27	15.62	38.91									
ECVF1549	Eagle Crags	116.97°	52.8	844.9	0.70664	0.7066	2.548	13.77	0.512491	–3	19.25	15.68	38.95									
ECVF1340	Eagle Crags	116.99°	91.1	435.4	0.70579	0.7056	4.421	22.12	0.512642	0	19.19	15.66	39.03									
ECVF1332	Eagle Crags	117.03°	145.8	38.20	0.70910	0.7063	2.893	17.36	0.512665	1	19.21	15.67	39.06	74.9	0.19	11.70	1.15	5.14	0.05			
ECVF1425	Eagle Crags	117.02°	35.2	742.3	0.70640	0.7064	4.887	36.41	0.512685	1	19.21	15.67	39.05	56.9	1.31	18.10	4.16	1.81	0.38			
ECVF1431	Eagle Crags	117.03°	48.6	560.1	0.70574	0.7057	4.796	23.66	0.512643	0	19.15	15.66	38.97	59.8	0.89	16.40	4.13	2.51	0.21			
pk914b*	Pilot Knob Valley	117.09°	5	553.6	0.70592	0.7059	3.951	16.39	0.512605	–1				50.9	1.19	18.31	3.39	0.51	0.21	209	0.81	
OPAL-2	Opal Mountain	117.15°	173.4	60.10	0.70946	0.7071	4.461	20.28	0.512646	0	19.25	15.62	38.93									
OPAL-4	Opal Mountain	117.15°	68.4	731.1	0.70708	0.7070	3.359	18.68	0.512414	–4												

TABLE 1. (*Continued*)

Sample	General locale	Long (W)	Rb	Sr	$\frac{^{87}Sr}{^{86}Sr}$	Sr_i	Sm	Nd	$\frac{^{143}Nd}{^{144}Nd}$	$\varepsilon_{Nd(t)}$	$\frac{^{206}Pb}{^{204}Pb}$	$\frac{^{207}Pb}{^{204}Pb}$	$\frac{^{208}Pb}{^{204}Pb}$	SiO_2	TiO_2	Al_2O_3	Na_2O	K_2O	P_2O_5	Ba	Zr/Ba	$\frac{La}{Yb_{(N)}}$
ECVF1514	Eagle Crags	117.20°	57.0	18.20	0.71201	0.7097	9.298	40.83	0.512697	1	19.29	15.68	39.03	77.2	0.09	12.40	4.25	4.30	0.03			
OM9313*	Barstow	117.26°	39.0	541.3	0.70504	0.7050	5.071	25.03	0.512513	–2				53.5	1.54	16.37	3.87	1.37	0.39	373	0.67	
OM9312*	Barstow	117.26°	33.0	445.1	0.70381	0.7038	5.618	20.37	0.513064	8				51.3	2.34	13.95	3.26	1.04	0.38	458	0.48	
pk914c*	Pilot Knob	117.29°	18.0	554.8	0.70527	0.7053	4.256	18.39	0.512713	2				52.5	1.30	15.25	3.05	1.19	0.25	380	0.57	
FP-13*	Fremont Peak	117.37°	12.9	358.7	0.70485	0.7048	3.260	12.74	0.512785	3	19.20	15.55	38.95	57.9	1.41	15.74	3.71	0.85	0.23			
FP-13I*	Fremont Peak	117.37°	10.7	494.0	0.70575	0.7057	3.370	12.19	0.512840	4	19.26	15.61	39.00	51.6	1.54	15.16	3.27	0.60	0.18			
FP-6Gi*	Fremont Peak	117.44°	180.4	236.1	0.70540	0.7047	4.476	18.82	0.512776	3	19.18	15.64	38.98	56.1	1.42	16.23	2.40	3.94	0.14			
FP-4*	Fremont Peak	117.46°		334.7	0.70501	0.7050	4.540	17.96	0.512833	4	19.12	15.59	38.88	52.5	1.85	16.76	3.42	1.02	0.25			
FP-1A*	Fremont Peak	117.46°	48.4	287.1	0.70523	0.7051	3.850	17.31	0.512657	1	19.24	15.61	39.03	60.4	1.10	16.61	3.27	2.22	0.19			
FP-1B*	Fremont Peak	117.46°	35.0	344.6	0.70513	0.7050	3.820	16.95	0.512721	2				59.6	1.06	16.71	3.14	1.65	0.20			
FP-1Bi*	Fremont Peak	117.46°	31.1	355.6	0.70496	0.7049	4.770	20.55	0.512698	1	19.21	15.61	39.03	58.3	1.47	17.22	3.46	1.19	0.21			
FP-10*	Fremont Peak	117.46°				0.7047					19.24	15.61	38.97	57.3	1.30	15.76	3.13	0.45	0.18			
FP-11*	Fremont Peak	117.47°	68.0	395.8	0.70476	0.7046	4.470	20.58	0.512731	2	19.18	15.60	38.99	61.6	1.39	17.07	3.26	2.64	0.27			
FP-11I*	Fremont Peak	117.47°	48.7	515.0	0.70408	0.7040	5.360	23.65	0.512815	4	19.17	15.59	38.96	52.0	2.36	17.76	3.39	1.55	0.35			
FP-5*	Fremont Peak	117.47°	51.5	269.0	0.70430	0.7041	3.800	14.47	0.512877	5	19.16	15.61	39.01	51.0	1.78	15.91	2.28	1.11	0.08			
FP-15*	Fremont Peak	117.48°	187.7	25.10	0.71280	0.7067	3.020	11.28	0.512662	1	19.35	15.62	39.07	74.8	0.00	15.44	3.61	5.50	0.00			
FP-12B*	Fremont Peak	117.48°	142.0	243.4	0.70667	0.7062	3.040	13.41	0.512617	0				68.4	0.73	17.23	2.16	2.54	0.18			
KRMR-4	Kramer Hills	117.57°	113.3	395.5	0.70650	0.7063	3.503	18.02	0.512615	0												
SA9311	Saddleback Butte	117.63°		263.9	0.70418	0.7042	3.404	12.28	0.512879	5												
SADL-1	Saddleback Butte	117.63°	8.2	275.4	0.70465	0.7046	3.601	13.25	0.512819	4				49.1	1.23	17.40	3.03	0.49	0.20	382	0.27	
EP9315	El Paso Mountains	117.85°		494.7	0.70443	0.7044	2.581	8.63	0.512780	3												

Notes: Major and trace element analyses were acquired by several different techniques. Some of the data in this table was originally published in Glazner (1990) and Miller and Miller (1991). See these studies for reference to analytical techniques. Major element, rare earth element (REE), and trace element data were obtained by commercial INAA (instrumental neutron activation analysis) except as noted by asterisks after the sample number. Analytical in-run precision (standard deviation of the number of analyses, generally four or five per run period) is generally better than 1% of the amount present for major elements and 10% of the amount present for trace elements, except Zr, which is better than 20% of the amount present. Routine analyses of common silicate-rock standards (e.g., G-2, AGV-1, RGM-1, QLO-1, SDC-1) run with these analyses gave results that match the accepted values within the error of the analyses. For Rb-Sr and Sm-Nd isotope analyses, 300–500 mg of whole-rock powder were dissolved in HF + HNO_3 mixture. Silicic samples were dissolved in Teflon (Parr) bombs at ~180 °C for 7 days. Mafic samples were dissolved in PFA Teflon (Savillex) vials at ~150 °C for 7 days. After dissolution, samples were aliquoted for Pb chemistry. Separation of Rb, Sr, and the REE group followed standard cation-exchange procedures. Nd and Sm were separated by using either HNO_3-CH_3OH chemistry on anion resin (cf. Faris and Warton, 1962) or alpha-hydroxyisobuturic acid chemistry on cation-exchange resin (cf. Eugster et al., 1970). Pb was separated by using an anion resin and HBr chemistry. Total procedure Pb blanks were less than 500 pg. Pb was analyzed in static multicollector mode with ^{206}Pb = 2V at filament temperatures between 1200 and 1400 °C; analyses are referenced to NBS 981 (common Pb) with $^{207}Pb/^{206}Pb$ = 0.91464 and corrected 0.10 ± 0.03%/amu (atomic mass unit) for fractionation. Total procedure blanks were less than 1 ng for Rb and Sr and less than 500 pg for Sm and Nd. Isotope data were acquired on a VG Sector 54 thermal ionization mass spectrometer. Sr and Nd were analyzed in dynamic-multicollector mode with ^{144}Nd = 1 V (Nd^+) and ^{88}Sr = 3 V. Rb and Sm were analyzed in static multicollector mode with ^{87}Rb = 200 mV and ^{147}Sm = 200–500 mV. Sr isotopic compositions are normalized to $^{86}Sr/^{88}Sr$ = 0.1194 and referenced to $^{87}Sr/^{86}Sr$ = 0.710250 (NBS 987). Nd isotopic compositions are normalized to $^{146}Nd/^{144}Nd$ = 0.7219 and referenced to La Jolla $^{143}Nd/^{144}Nd$ = 0.511850. External reproducibility of standards remained better than ±0.000020 (2 s.d.) for Sr and ±0.000005 (2 s.d.) for Nd over the course of the analyses, which took place between 1993 and 1997. Analysis of BCR-1 at the University of North Carolina using our mixed Sm/Nd tracer gave $^{143}Nd/^{144}Nd$ = 0.512627, Sm = 6.581, and Nd = 28.71. Sr_i and $\varepsilon_{Nd(t)}$ indicate initial $^{87}Sr/^{86}Sr$ and $^{143}Nd/^{144}Nd$ isotopic compositions at the crystallization age. Epsilon values for Nd at crystallization age ($\varepsilon_{Nd(t)}$) are calculated by using $^{143}Nd/^{144}Nd_{(CHUR,\ 0\ Ma)}$ = 0.512638 and $^{147}Sm/^{144}Nd_{(CHUR,\ 0\ Ma)}$ = 0.1967. Ages of the rocks in this study range from ca. 20 to 17 Ma. Initial ratios are calculated by assuming an age of 20 Ma for all samples.

*Major and trace elements analyses were done by DCP (direct coupled plasma) spectrometry at the University of North Carolina.

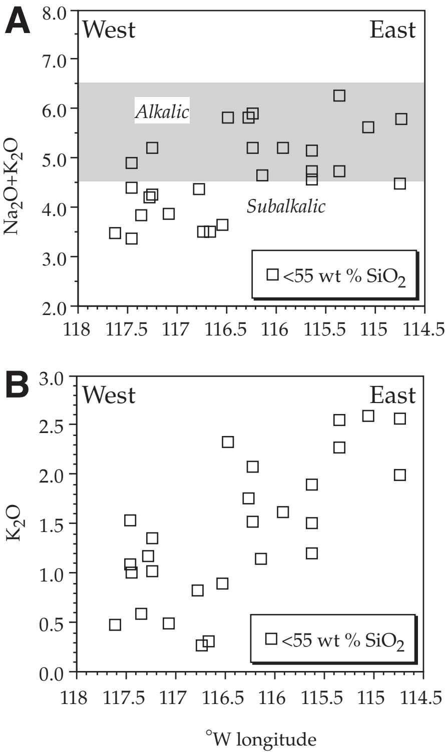

Figure 2. (A) Plot of total alkalis vs. °W longitude for mafic rocks from the study area. Mafic rocks east of 116°W are all alkalic whereas most mafic rocks from west of this longitude have subalkalic chemistry. Note that boundary between alkalic and subalkalic is not sharp in this plot because rock types range from 48 to 55 wt% SiO_2. (B) Plot of K_2O vs. °W longitude, showing that alkalic chemistry of basalts to the east is primarily due to increase in K_2O from west to east.

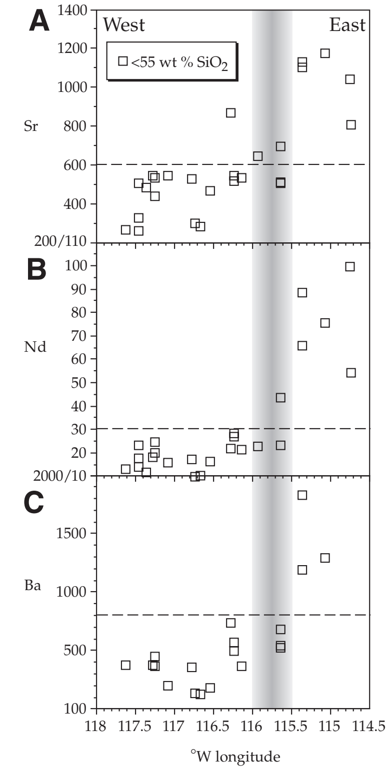

Figure 3. Variation in Sr, Nd, and Ba contents of mafic rocks with °W longitude. Marked increases in concentration (inflections in the trend) for these elements occur between ~116°W and 115.5°W (gray band). Dashed lines show approximate maximum values for rocks west of 116°W (oceanic domain). See text for further discussion. One sample (a-3) from the Avawatz Mountains is not shown on this plot because it falls significantly off the east-west line and west of the 116°W break. This sample has chemical and isotopic characteristics similar to those east of 116°W; thus we suggest that the break may project up toward the east end of the Garlock fault and southern extension of the Death Valley fault zone. Compare with Figure 1.

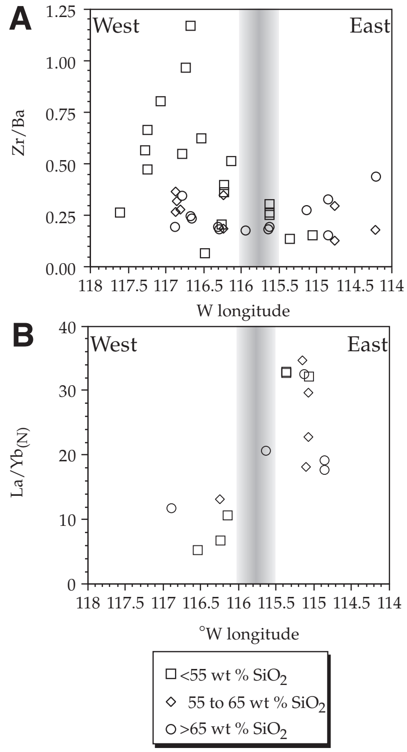

Figure 4. Variation in (A) Zr/Ba and (B) $La/Yb_{(N)}$ with °W longitude for all bulk compositions. Gray band as in Figure 3. Zr/Ba shows high degree of scatter west of 116°W but is uniformly less than 0.27 east of this longitude. Variations in this ratio in the mafic rocks will be affected by source differences and crustal contamination. Crustal contamination will generally lower the ratio since most crustal rocks have Zr/Ba ratios much lower than most basalts. $La/Yb_{(N)}$ (Fig. 2B) shows high degree of LREE enrichment in mafic rocks east of 116°W. Normalization from Sun and McDonough (1989).

Basu, 1995). A depleted-mantle source for the western part of the study area is also supported indirectly by Nd data on metabasalts in the Pelona-Orocopia-Rand schists. Two metabasalt analyses from the schists reported in Miller et al. (1996) have $\varepsilon_{Nd(t)} > +8$. Assuming that these basalts are representative of the oceanic crust of the schists, then mantle lithosphere and asthenosphere beneath the basaltic basement of the schists must also have had relatively high $\varepsilon_{Nd(t)}$, consistent with the Miocene data. Later in this paper, the possible extent of the Pelona-Orocopia-Rand schists at depth in the crust is discussed more.

East of 116°W. The extrapolated Sr_i and $\varepsilon_{Nd(t)}$ values for the mantle source east of 116°W are greater than 0.706 and generally less than –4, respectively, and thus quite different from the Sr and Nd isotopic composition of mantle in the central and western Mojave Desert. These values ($Sr_i > 0.706$ and $\varepsilon_{Nd(t)} < -4$) are similar to those from lithospheric mantle–derived basalts in southern Nevada and westernmost Arizona (e.g., Farmer et al., 1989; Bradshaw et al., 1993; Feuerbach et al., 1993). Thus, the contamination versus longitude trends would seem to indicate that two distinct mantle isotopic sources were present in the early Miocene along the transect with a significant boundary at or about 116°W. This indication is also consistent with the trace element data and reinforces the observation that, at least for mantle structure, there is not a continuous transition across the Mojave, as originally hypothesized by Glazner and O'Neil (1989).

Because Proterozoic rocks are widespread in surface outcrops east of 116°W (e.g., Wooden and Miller, 1990), it could be argued that these extrapolations are not valid. Crustal assimilation of Proterozoic crust by a depleted-mantle–derived basalt could produce fairly dramatic shifts in isotopic composition with minor changes in SiO_2 content (Figs. 7 and 9; e.g., Hildreth and Moorbath, 1988; Cribb and Barton, 1996). High rates of initial assimilation by basalt intruding the crust, with little change in SiO_2, have also been postulated on the basis of heat-balance arguments (Reiners et al., 1995) and could especially alter the isotopic composition of depleted basalts intruded into Proterozoic crust. Hence the contamination problem for the mafic rocks, especially those east of 116°W, bears more examination.

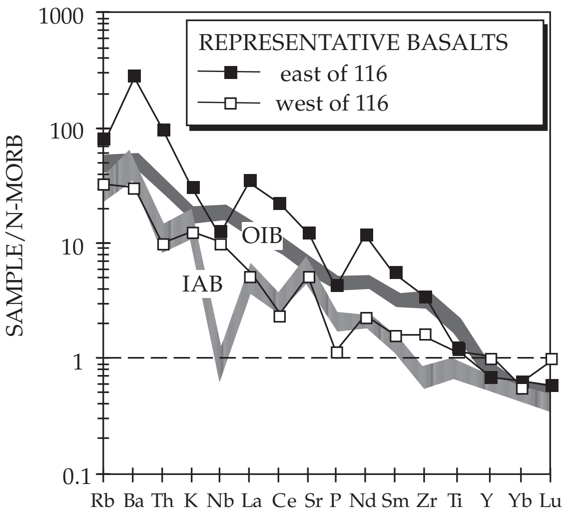

Figure 5. Multielement-normalization plot for representative basalts from east and west of 116°W longitude. Sample from east of 116°W longitude is SV-2 (Table 1). Sample from west of 116°W longitude is ALVO-3. Both basalts are enriched relative to N-MORB, but LILE and LREE enrichments are up to 10× higher in SV-2. Note also that SV-2 has a modest negative Nb anomaly not seen in ALVO-3. Samples are normalized to N-MORB of Sun and McDonough (1989). Also shown are typical patterns for calc-alkalic arc basalt and ocean-island basalt from data in Wilson (1989). OIB—oceanic-island basalt, IAB—island-arc basalt.

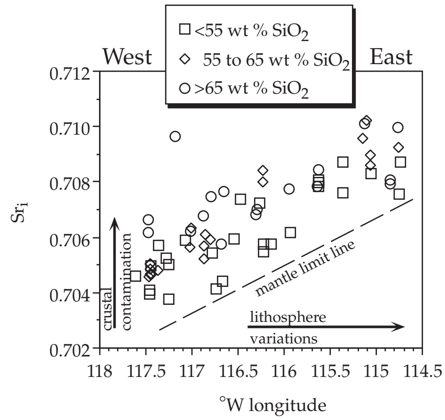

Figure 6. Variation in Sr_i with °W longitude for all bulk compositions. Vertical scatter in Sr_i is due primarily to contamination, but even with scatter, Sr_i increases from west to east for all bulk compositions. Spread in Sr_i of mafic rocks at any given longitude is ~0.0015, whereas spread from west to east is ~0.004. Lower limit lines define possible mantle variability from west to east across study area. Arrows show that scatter is a combination of lithosphere variations and crustal contamination. Inflections in Sr_i with °W longitude as seen in trace element data are not apparent on this diagram. See text for further discussion.

The P_2O_5/K_2O ratios of basalts have been shown to be a good indicator of crustal contamination when plotted against an index of differentiation and/or isotopic composition (e.g., Carlson and Hart, 1987; Glazner and O'Neil, 1989; Farmer et al., 1995). Crustal rocks and crust-derived melts have P_2O_5/K_2O ratios near 0, and mantle-derived basalts generally have ratios of ≥0.4 (e.g., Wilson, 1989); thus the ratio P_2O_5/K_2O is highly sensitive to crustal contamination. Furthermore, the P_2O_5/K_2O ratio of basalts is unaffected by either crystal fractionation of near-liquidus phenocrysts or by the degree of partial melting of the source, because K and P behave incompatibly in both processes. Figure 11 plots P_2O_5/K_2O versus Sr_i and $\varepsilon_{Nd(t)}$ for mafic rocks with <55 wt% SiO_2 and >5.5 wt% MgO. Crustal contamination is clearly indicated by the low P_2O_5/K_2O ratios of many of the mafic rocks from across the study area, even those with relatively high MgO contents. However, several samples have $P_2O_5/K_2O \geq 0.4$ over the full range of Sr_i and $\varepsilon_{Nd(t)}$ and longitude. These samples show minimal contamination; thus their isotopic compositions are most likely to reflect the mantle from which they were derived.

For samples west of 116°W (i.e., 116°W to 117°W and west of 117°W), there is complete overlap in the data, including the samples with high P_2O_5/K_2O ratios. The scatter in the data for these samples with high P_2O_5/K_2O ratios may also indicate that there is some true isotopic heterogeneity in the mantle source of these rocks.

Samples east of 116°W are separated from the data to the west (Fig. 12). The two samples east of 116°W, with high Sr_i and low $\varepsilon_{Nd(t)}$ values and high P_2O_5/K_2O ratios (SV-2 and A3-1; Table 1), have the lowest SiO_2 (true nepheline-normative basalts) of all the samples plotted in Figures 7A and 9A, which suggests that our contamination extrapolation is valid. We have also plotted data for synextensional early Miocene basaltic rocks from the Colorado River trough (Bradshaw et al., 1993) in Figure 11, and it is apparent that several of these samples are also crustally contaminated. Two of the samples from Bradshaw et al. (1993) plot off the diagram at high P_2O_5/K_2O ratios (Fig. 11). These two samples, like the two samples with high P_2O_5/K_2O ratios from our study, have the lowest SiO_2 within their data set and are thus were also derived from mantle characterized by high Sr_i and low $\varepsilon_{Nd(t)}$.

The isotopic characteristics of contaminated basalts east of 116°W could be generated by mixing basalt having low Sr_i and high $\varepsilon_{Nd(t)}$ with modest amounts of probable lower- or upper-crustal rocks, as shown by the mixing curves in Figure 11. The resultant changes in SiO_2 content (Fig. 11) are too high for upper crust but not for relatively small mixtures of depleted basalt with lower crust. However, the simple mixing models fail to account for the high LILE and LREE abundances in both the uncontaminated and contaminated samples. Sr and Nd concentrations for model mixtures (Fig. 11) are too low for these samples (Fig. 3 and Table 1).

Assimilation of a silicic anatectic melt by a depleted basalt is also unlikely to explain the trace element characteristics of the basalts with low P_2O_5/K_2O ratios east of 116°W because Sr behaves compatibly in most crustal-melting situations. Anatectic melts should therefore have low Sr, whereas these rocks all have high Sr (Fig. 3). High rates of assimilation relative to crystallization in the deep crust could possibly elevate the Sr and Nd concentrations in the basaltic magmas while lowering $\varepsilon_{Nd(t)}$ and raising Sr_i, if incompatible behavior for both Sr and Nd is assumed. Given that the uncontaminated, nepheline-normative basalts with high P_2O_5/K_2O ratios east of 116°W have the highest Sr and Nd (and highest LILE and LREE contents generally; Table 1), it is unlikely that the contaminated basalts with low P_2O_5/K_2O ratios east of 116°W acquired their elevated LILE and LREE abundances by a completely different process (i.e., deep-crustal AFC [assimilation coupled with fractional crystallization]). Instead, the high LILE and LREE contents and the high Sr_i and low $\varepsilon_{Nd(t)}$ isotopic characteristics for all mafic rocks east of 116°W (uncontaminated and contaminated) primarily reflect the mantle signature. The lower LILE and LREE contents for contaminated mafic rocks are produced by mixing the

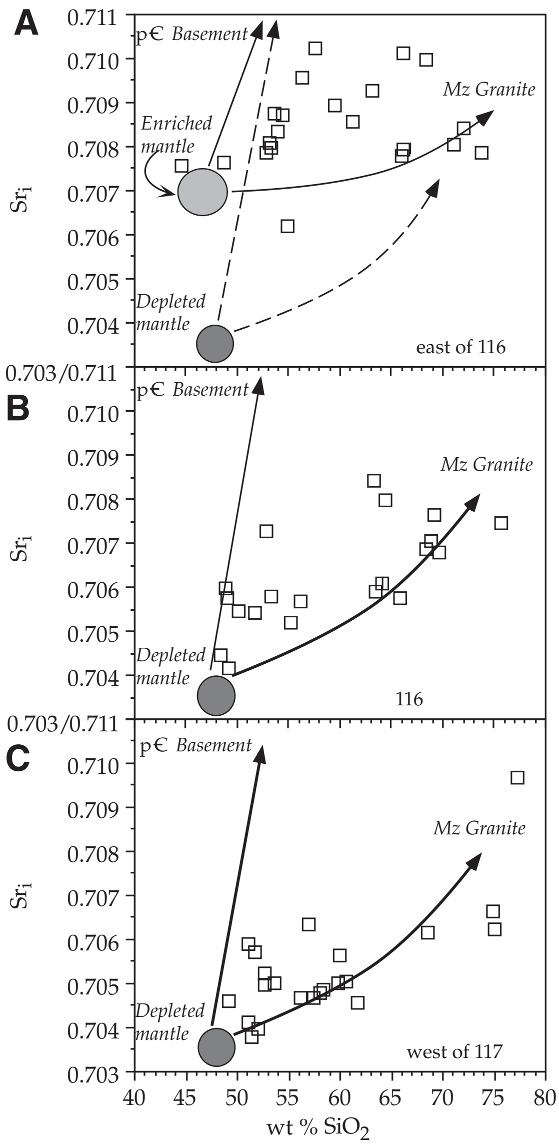

Figure 7. Variation in Sr_i with SiO_2 for rocks (A) east of long 116°W, (B) between long 116°W and 117°W, and (C) west of long 117°W. Basalts from east of 116°W come from enriched mantle with $Sr_i > 0.7065$. Compare with Figure 1. Basalts west of 116°W derived from depleted mantle. Increase in Sr_i with SiO_2 indicates that open-system contamination is important in producing compositional variation in the Tertiary volcanic fields regardless of longitudinal positions. Mixing occurs by a variety of processes including bulk assimilation, magma mixing, and assimilation coupled with fractional crystallization (AFC). Mixing trajectories for typical Precambrian basement and Mesozoic granite are primarily for illustrative purposes; Sr isotopic compositions for crustal end members vary significantly. Compare with Figure 6.

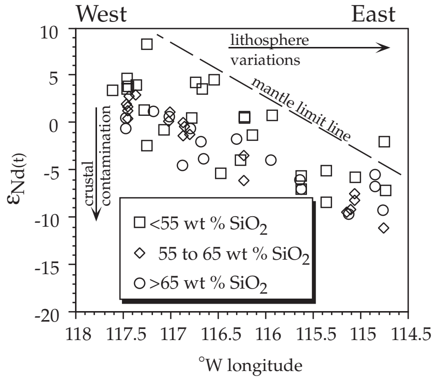

Figure 8. Variation in $\varepsilon_{Nd(t)}$ with °W longitude for all bulk compositions. As in Figure 6, vertical scatter is due largely to contamination effects, whereas horizontal trends reflect lithosphere variations. $\varepsilon_{Nd(t)}$ decreases from west to east, but again no inflections are apparent in the data. Upper limit line for mantle as in Figure 6. Spread in $\varepsilon_{Nd(t)}$ values from west to east is about 17. See text for further discussion.

LILE- and LREE-enriched basalts with crust having lower LILE and LREE contents.

Mantle xenoliths from post-Miocene basalts in the Mojave Desert support our conclusions regarding Miocene mantle variation. Several post-Miocene basalt cones from the Mojave Desert bear mantle xenoliths (Wilshire et al., 1988). Among these xenolith suites, peridotite xenoliths with hydrous phases, LILE enrichments, and high Sr_i and low $\varepsilon_{Nd(t)}$ isotope ratios typical of enriched mantle are found only east of 116°W (Wilshire et al., 1988; Mukasa and Wilshire, 1997), whereas mantle xenoliths from the western Mojave Desert are all anhydrous peridotites with depleted-mantle geochemical characteristics (Wilshire et al., 1988).

Eastern Mojave Enriched Mantle. The age and mechanism of the mantle enrichment east of 116°W remain somewhat cryptic. Bradshaw et al. (1993) postulated that enrichment of subcontinental mantle beneath the Colorado River trough occurred at ca. 1.6 Ga because their Pb data lie on an ~1.6 Ga Pb-Pb secondary "isochron." Given the near ubiquity of contamination in these rocks and the extreme sensitivity of Pb isotopes to contamination, the secondary "isochron" of Bradshaw et al. is difficult to evaluate. Bradshaw et al. (1993) did not screen the data used to construct their secondary Pb-Pb isochron for contamination, but much of the crustal growth in the Mojave and western Arizona occurred between 1.7 and 1.6 Ga (e.g., Wooden and Miller, 1990). It may be that significant modification of the mantle also occurred at this time.

Longitudinal variation of whole-rock Pb isotopes for basalts with MgO > 6 wt% (from this study) is similar to all the Pb data where $^{206}Pb/^{204}Pb$ decreases eastward and $^{208}Pb/^{204}Pb$ increases eastward (Fig. 10; note that three of these basalts have $P_2O_5/K_2O < 0.3$, but we lack Pb data on these, so MgO is used to try to distinguish least contaminated samples). For any given $^{206}Pb/^{204}Pb$ ratio, the high-MgO basalts east of 116°W also have high $^{207}Pb/^{204}Pb$ and $^{208}Pb/^{204}Pb$ ratios. Thus even in the least contaminated basalts for which we have Pb data, the Pb isotopic signatures appear to show a change from west to east that may partly reflect mantle variation. Too few data on uncontaminated basalts east of 116°W are available to infer whether this trend is real, but it is noteworthy that the Pb isotopic compositions reported by Farmer et al. (1989), Feuerbach et al. (1993), and in Bradshaw et al. (1993) for uncontaminated nepheline- and hypersthene-normative Miocene basalts from southern Nevada are similar to those reported here. This consistency lends support to our inference that the Pb isotopic characteristics of the least contaminated mafic rocks east of 116°W may reflect mantle.

The data from this study and that of Farmer et al. (1989), Bradshaw et al. (1993), and Feuerbach et al. (1993) collectively imply that, prior to Miocene extension, much of the present-day southern Great Basin and eastern Mojave was underlain by ancient mantle lithosphere capable of producing mafic magmas with similar geochemical characteristics—high LREE and Sr concentrations, low $\varepsilon_{Nd(t)}$ values (<–4 or so), high Sr_i values (≥0.707), and high $^{208}Pb/^{204}Pb$

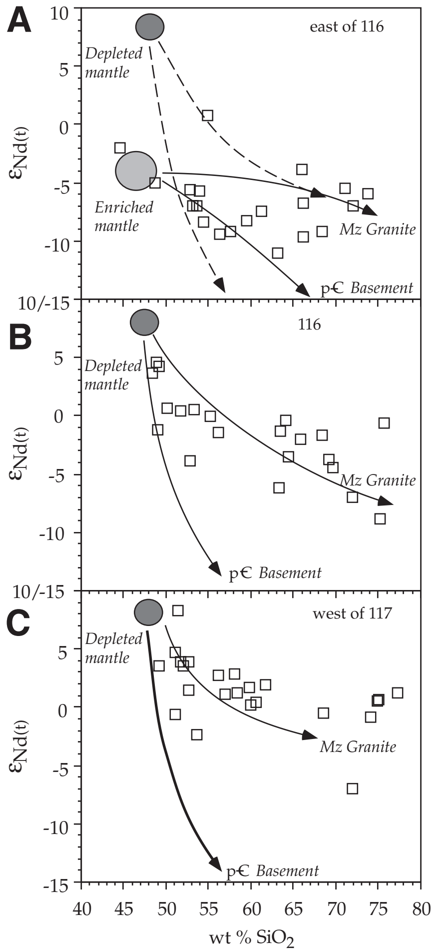

Figure 9. Variation in $\varepsilon_{Nd(t)}$ with SiO_2 for rocks (A) east of long 116°W, (B) between long 116°W and 117°W, and (C) west of long 117°W. Decrease in $\varepsilon_{Nd(t)}$ with increasing SiO_2 indicates that open-system contamination is important in petrogenesis of the Tertiary volcanic rocks. Compare with Figure 7. In A, for the area east of long 116°W, a low-$\varepsilon_{Nd(t)}$ (=–2) enriched-mantle end member is inferred. In B and C, for the area west of long 116°W, a higher-$\varepsilon_{Nd(t)}$ (>+4) depleted-mantle end member is inferred. As in Figure 7, mixing curves are for illustrative purposes; Nd isotopic compositions for crustal end members vary significantly, especially Mesozoic granites. Compare with Figure 8.

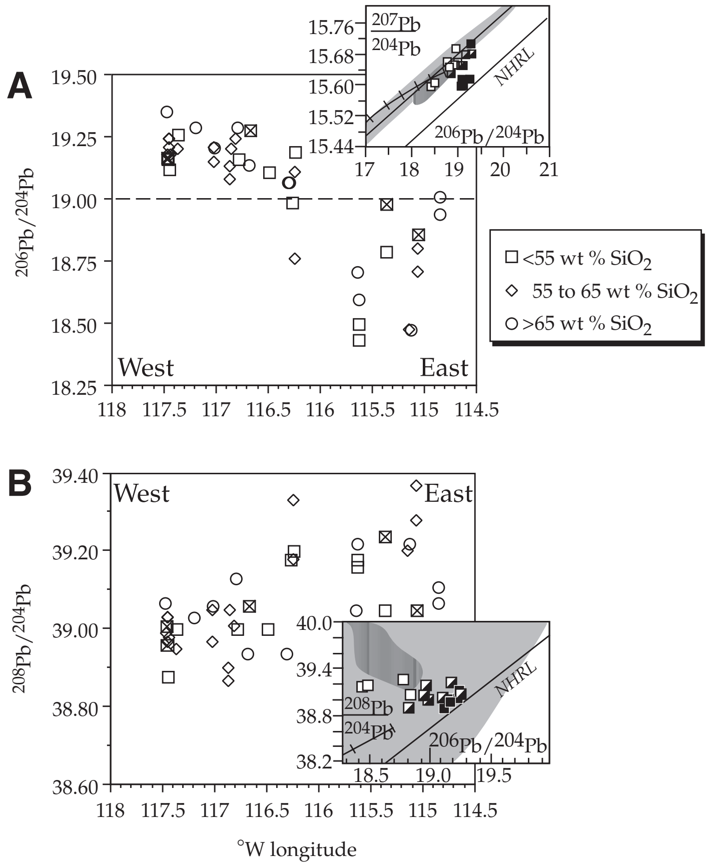

Figure 10. Variation in (A) whole-rock $^{206}Pb/^{204}Pb$ and (B) whole-rock $^{208}Pb/^{204}Pb$ with °W longitude. $^{206}Pb/^{204}Pb$ generally decreases from west to east for all bulk compositions, whereas $^{208}Pb/^{204}Pb$ increases from west to east. $^{206}Pb/^{204}Pb$ values are generally more scattered with eastward position. Mafic samples with Xs have MgO > 6 wt%. West of 116°W, the range of $^{206}Pb/^{204}Pb$ values is relatively restricted, and most values > 19.0. Increasing scatter toward the east is probably due to contamination of magmas with basement that is more isotopically heterogeneous to the east (Mojave Precambrian crust); however, as shown in B, this basement is also characterized by uniformly high $^{208}Pb/^{204}Pb$. Insets show variations of (A) $^{207}Pb/^{204}Pb$ vs. $^{206}Pb/^{204}Pb$ and (B) $^{208}Pb/^{204}Pb$ vs. $^{206}Pb/^{204}Pb$ for mafic rocks; white symbols are for mafic rocks east of long 116°W, half-filled symbols for mafic rocks between long 116°W and 117°W, and black symbols for mafic rocks west of long 117°W. NHRL is Northern Hemisphere reference line of Hart (1984) for Northern Hemisphere oceanic basalts. Curve is the Stacey and Kramers (1975) average crust model with 0.5 Ga increments marked by ticks. Gray shaded field is Mojave data array for Precambrian whole-rock and Mesozoic feldspar Pb, and line through this field is 1.75 Ga secondary isochron (Wooden et al., 1988; Wooden and Miller, 1990). Ruled field shows range of whole-rock Pb for lower-crustal xenoliths from the Old Woman Mountains area (Hanchar et al., 1994). Moving from west to east, mafic rocks trend progressively away from oceanic Pb values to values typical of eastern Mojave lithosphere. Data from east of long 116°W lie approximately along the 1.75 Ga secondary isochron of Wooden and Miller (1990), but the range of values is fairly restricted. Note that there is a wide range of $^{208}Pb/^{204}Pb$ values for eastern Mojave Pb and that most plot above the Stacey and Kramers (1975) growth curve even though field (gray shaded area) extends to below NHRL.

and $^{207}Pb/^{204}Pb$ ratios for any given $^{206}Pb/^{204}Pb$. Given that these areas are also where Proterozoic crust ("Mojavia") with unique Nd and Pb isotopic characteristics is found (Bennett and DePaolo, 1987, Wooden et al., 1988), it is possible that this mantle may be uniquely associated with Mojavia, as suggested by earlier studies (Farmer et al., 1989; Livicarri and Perry, 1993). It may be that Precambrian mantle domains closely covary farther to the east of the present study, across the transition from Mojavia to Proterozoic crust of the Yavapai and Mazatzal terranes of Arizona (Karlstrom and Bowring, 1988). Future work is required to test this hypothesis.

The 116°W Break: A Crustal Boundary Also?

We have argued herein that the mantle source east of 116°W was different from rocks west of this longitude when these rocks were erupted,

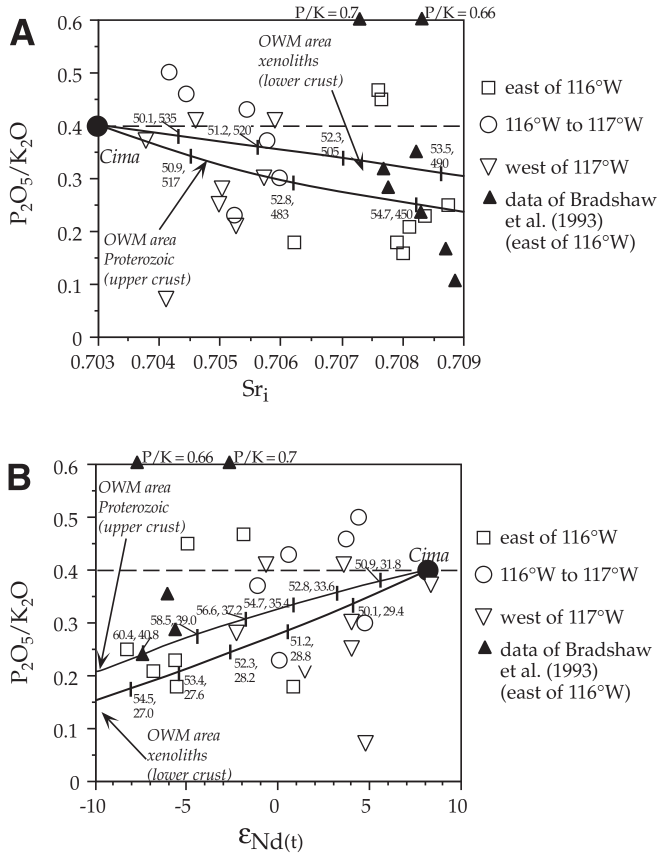

Figure 11. P_2O_5/K_2O vs. (A) Sr_i and (B) $\varepsilon_{Nd(t)}$ for mafic rocks from across the study area. Note that these symbols differ from those in other data plots and Figure 1. Samples falling above $P_2O_5/K_2O = 0.4$ (dashed line) are the least contaminated with crustal material. Most rocks plot below this line, probably indicating some contamination with crust. Data from Colorado River trough from Bradshaw et al. (1993) also given for comparison. Also shown are mixing curves for depleted-mantle basalt (Cima; Farmer et al., 1995) and two probable crustal end members: Proterozoic lower crust (Hanchar et al., 1994) and Old Woman Mountains Proterozoic rocks (Miller and Wooden, 1994). Tick marks indicate 10% mixing increments, and numbers next to curves give SiO_2 and (A) Sr and (B) Nd contents in the mixtures. Mixing parameters are as follows: Cima basalt has 550 ppm Sr, 30 ppm Nd, $Sr_i = 0.703$, $\varepsilon_{Nd(t)} = +8$, $P_2O_5/K_2O = 0.4$, and $SiO_2 = 49$ wt%; lower-crust end member has 412 ppm Sr, 24 ppm Nd, $Sr_i = 0.7136$, $\varepsilon_{Nd(t)} = -17$; $P_2O_5/K_2O = 0.03$; $SiO_2 = 59$ wt%; Proterozoic upper-crust end member has 216 ppm Sr, 48.4 ppm Nd, $Sr_i = 0.7390$, $\varepsilon_{Nd(t)} = -17.9$, $P_2O_5/K_2O = 0.07$, $SiO_2 = 68.3$ wt%. Simple mixing of Cima-like basalt with typical Proterozoic crust cannot produce the enriched trace element signatures of the mafic rocks east of 116°W, even those that are contaminated and have $P_2O_5/K_2O < 0.3$. See text for discussion.

but is there any obvious crustal expression of this boundary, either in the surface geology or in the isotopic data? East of 116°W, Precambrian basement is widespread (Fig. 1). Thus it is not surprising that isotopic compositions of intermediate-composition and silicic rocks east of this longitude also have isotopic signatures that, like the mafic rocks, reflect an old lithosphere—generally Sr_i >0.708 and $\varepsilon_{Nd(t)} < -7$ (Table 1; Fig. 1), and eastern Mojave Pb signatures (e.g., Fig. 10; Wooden et al., 1988). These signatures clearly reflect input from Precambrian crust (Wooden and Miller, 1990) or Mesozoic granitoids derived from Precambrian crust (Miller and Wooden, 1994).

Isotopic signatures of intermediate-composition and silicic rocks just west of 116°W (i.e., Cady Mountains and vicinity) considerably overlap those to the east of this longitude (Fig. 1) and imply that Precambrian crust extends farther west than 116°W. The 116°W break does not therefore coincide with the craton margin on the basis of isotopic data even though it does mark the edge of the Proterozoic North American lithospheric mantle when these rocks were erupted. This interpretation would be consistent with the position of the craton margin (hinge line of Fig. 1) based on Paleozoic stratigraphy and scattered exposures of Precambrian basement near Victorville (Martin and Walker, 1992). Also, zircons from Mesozoic plutons in the Barstow area (Boettcher and Walker, 1993) and the Miocene Waterman Hills granodiorite (Walker et al., 1995) show Precambrian inheritance, which indicates the presence of some Precambrian basement in the crust well to the west of 116°W.

The main crustal contributor to the intermediate-composition and silicic rocks west of 116°W may not, however, have been Precambrian basement. Glazner and O'Neil (1989) noted that there appears to be a break in the $\delta^{18}O$ data for silicic volcanic rocks at about 116°W. Silicic rocks west of this longitude have high $\delta^{18}O$ values, implying source materials significantly different from similar rocks east of this longitude. Glazner and O'Neil (1989) hypothesized that the underthrust oceanic Pelona-Orocopia-Rand schists served as a crustal source for Miocene silicic rocks erupted west of this longitude (including those in the Cady Mountains just referred to). The Pelona-Orocopia-Rand schists are characterized by high $\delta^{18}O$ values and thus represent the most likely source materials for the silicic rocks from west of this longitude. Intermediate-composition and silicic rocks that were erupted through the area where Rand schists and eugeoclinal rocks crop out also have Sr_i, $\varepsilon_{Nd(t)}$, and Pb isotopic signatures that reflect relatively young, more oceanic-like lithosphere (Fig. 1), in agreement with the data from the earlier study by Glazner and O'Neil (1989). The $\delta^{18}O$ data also support our general inferences about mantle sources east and west of this longitude, because the mantle beneath the Pelona-Orocopia-Rand schists is depleted oceanic mantle (Miller et al., 1996).

It is interesting that earlier workers (Darton et al., 1915; Bassett and Kupfer, 1964; Hamilton and Myers, 1966) noted that there appear to be surface physiographic expressions of a geologic boundary (lineament) at about where we place our mantle isotopic discontinuity. East of this longitude, many of the mountain ranges (e.g., Old Woman Mountains, Piute Range, Providence Mountains; cf. Jennings, 1977) trend more northward or northeastward as in the classic Basin and Range of Nevada. West of this longitude, the ranges of the central and western Mojave have no dominant trend and are separated by numerous right-lateral faults (Bassett and Kupfer, 1964). Hamilton and Myers (1966) and Stewart and Poole (1974) suggested that the Death Valley fault zone may project into southeastern California at ~116°W longitude with 50 to 80 km of right-lateral displacement, but

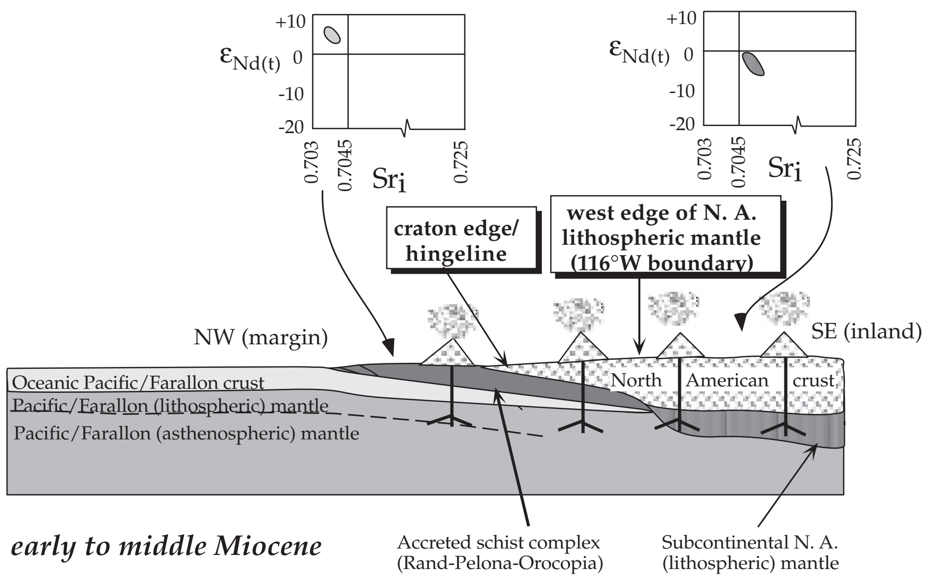

Figure 12. Cartoon cross section showing inferred lithospheric structure from west to east across the study area during the early to middle Miocene. Sr-Nd diagrams show variation in mantle source of basalts from west to east that is used to infer mantle lithospheric structure. The mantle lithosphere beneath the western Mojave was likely thin (5-10 km), given the young age of the Farallon plate at this latitude in early Miocene time (less than 5 m.y.; cf. Severinghaus and Atwater, 1990; Dickinson, 1997). No scale is implied, and we can only infer the presence of mantle lithosphere and not the thickness beneath the eastern part of the study area during the early Miocene. Note the extension of the thinned continental margin beyond the inferred west edge of the continental North American mantle lithosphere. See text for discussion.

Davis (1977) showed that fault and stratigraphic relationships do not support these large displacements. Nevertheless, the lineament proposed by Bassett and Kupfer (1964) is coincident with our proposed isotopic break, and modern-day seismicity is also more common to areas west of this longitude (Goter et al., 1994; Miller and Glazner, 1997). It may be that this longitude marks a transition in the overall strength of the lithosphere owing to the presence of Pelona-Orocopia-Rand schists in the crustal column to the west of 116°W.

The data from this study and the $\delta^{18}O$ data from Glazner and O'Neil (1989) allow us to construct a fairly detailed cartoon cross section of the early Miocene crust and mantle along our transect (Fig. 12). Precambrian crust was present west of 116°W, at least to the longitude of Barstow (Fig. 1), but by early Miocene time was thinned and underlain by Pelona-Orocopia-Rand schists and oceanic mantle, which served as the main crustal source for silicic melts and/or the main contaminant for depleted basalts rising from the mantle. Some contribution from Precambrian crust and immature arc-like crust of the eugeocline is also inferred. East of 116°W, Precambrian crust was more abundant and served as the main source for silicic rocks and/or was the main contaminant of enriched basalts rising from the North American mantle. No Pelona-Orocopia-Rand schists were (or are) present in the lithosphere East of this boundary. An important corollary of this study and the previous study by Glazner and O'Neil (1989) is that 116°W marks the eastern limit of crustal underplating and appreciable stripping of subcrustal lithospheric mantle by the Pelona-Orocopia-Rand schists at the latitude of our transect. Our findings thus reinforce previous work that has suggested that low-angle Late Cretaceous–early Tertiary subduction of the Farallon plate did not completely remove the North American mantle lithosphere (Livicarri and Perry, 1993; Ducea and Saleeby, 1998).

Where Is the $Sr_i = 0.706$ Line in the Mojave?

The $Sr_i = 0.706$ isopleth was originally defined by Kistler and Peterman (1973) as an isotopic boundary marking the western edge of autochthonous Precambrian basement (either exposed or at depth) in the western Cordillera of the United States. The data used by Kistler and Peterman (1973, 1978) and Kistler (1990) to define the $Sr_i = 0.706$ line mostly come from Mesozoic granitoid rocks in Nevada and eastern California (the Sierra Nevada batholith). That the $Sr_i = 0.706$ line marks the western edge of Precambrian basement (autochthonous North America) in the western Cordillera is still one of the most widely embraced ideas in western Cordilleran paleogeography and paleotectonics, but this definition has been difficult to apply to the Mojave Desert region since it was originally proposed (e.g., Kistler and Peterman, 1978; Glazner and O'Neil, 1989).

Kistler and Peterman (1978) originally suggested that most of the Mojave Desert lay inboard of the $Sr_i = 0.706$ line and, by inference, was underlain by Precambrian basement, except for a thin (maximum of 30 km width) corridor in the northern Mojave Desert and southernmost Sierra Nevada. Kistler and Peterman (1978) proposed that this thin corridor, with rocks having $Sr_i < 0.706$, was the site of a late Precambrian rift in the Precambrian basement of the Mojave Desert. Glazner and O'Neil (1989) concluded that the gradual eastward increase in Sr_i was incompatible with the rift proposed by Kistler and Peterman (1978), although subsequent work by Miller et al. (1995) has shown that plutons within this zone have wide-ranging and age-dependent Sr, Nd, and Pb isotopic compositions. Kistler (1990) later proposed that much of the western Mojave Desert was not underlain by Precambrian crust but was instead underlain by allochthonous oceanic and metasedimentary basement (termed "Panthalassan" lithosphere). Mesozoic plutons derived from or intruded into the area inferred to be underlain by Panthalassan basement are characterized by radiogenic Sr ($Sr_i \geq 0.706$) and high $\delta^{18}O$ values (Masi et al., 1981; Kistler, 1990) and, in some cases, by strongly peraluminous geochemical compositions (Miller et al., 1996). This Panthalassan lithosphere was interpreted to include areas underlain by Pelona-Orocopia-Rand schists, but the eastern edge of Panthalassan lithosphere as defined by Kistler (1990) was well west of where our data and the data of Glazner and O'Neil (1989) indicate that Pelona-Orocopia-Rand schists are present at depth.

Coleman and Glazner (1997) have argued that, because much of the eastern Sierra Nevada batholith was generated from subcontinental lithospheric mantle in the Cretaceous (Coleman et al., 1992, 1995; Sisson et al., 1996), the $Sr_i = 0.706$ line more accurately delineates the western limit of the Precambrian continental lithospheric mantle and not the western limit of Precambrian crust. If we apply this same definition to the Mojave Desert, then the $Sr_i = 0.706$ line would correspond to the isotopic break at 116°W. Proterozoic

North American basement extends farther west than 116°W, but Proterozoic North American mantle does not (at the latitude of our transect). The position of the Sr_i = 0.706 line by this definition is also valid in the Mesozoic rocks of the Mojave Desert. The mantle source for Mesozoic plutons west of 116°W in the Mojave Desert was depleted mantle (Miller and Glazner, 1995). East of 116°W, the mantle source for Mesozoic plutons was demonstrably Precambrian continental lithospheric mantle (Young et al., 1992; Miller and Wooden, 1994).

Tectonic Causes of Miocene Volcanism in the Mojave

The underlying cause or causes of volcanism in the Mojave Desert during this time period remain elusive. The most recent models for the southern Basin and Range (including the eastern Mojave Desert) propose that volcanism was a consequence of adiabatic decompression melting of volatile-enriched continental lithospheric mantle in response to uplift and tectonic extension (Bradshaw et al., 1993; Hawkesworth et al., 1995).

Development of extension-driven models is motivated by the frequent observation that volcanism in many parts of the Basin and Range commenced with eruption of modest volumes of enriched, pre- or synextensional, lithospheric mantle–derived basalt and ended with small volumes of depleted, postextensional, asthenospheric mantle–derived basalt (e.g., Farmer et al., 1989; Daley and DePaolo, 1992; Leeman and Harry, 1993; Feuerbach et al., 1993; Bradshaw et al., 1993; Davis and Hawkesworth, 1995). In these models, convective thinning of the lower lithosphere following homogeneous lithosphere thickening (e.g., Houseman et al., 1981; Platt and England, 1993) results in extension and decompression melting of the lithospheric mantle to produce enriched basalts. Asthenospheric basalts are subsequently erupted as extension continues and the melting isotherms migrate upward (e.g., Leeman and Harry, 1993; Platt and England, 1993; Hawkesworth et al., 1995).

Whether all aspects of this model can be applied to the entire Mojave Desert is questionable. Across the study area, the amount and spatial distribution of pre-Tertiary crustal thickening and contractile deformation were variable. Some areas of Cenozoic extension and magmatism crudely coincide with areas of Mesozoic shortening (e.g., Howard and John, 1987; Howard et al., 1987; Glazner et al., 1989); other areas do not (e.g., Cady Mountains, Glazner, 1988). Convective thinning and extension-driven magmatism models imply a close spatial relationship between extension and volcanism. However, if the crust is inherently weak, then extension of the Mojave Desert lithosphere could also have resulted from the instability of the Mendocino triple junction as it passed northward through Mojave Desert latitudes (e.g., Ingersoll, 1982; Glazner and Bartley, 1984) and thus may not require thickening to undergo extension.

More problematic for extension-driven volcanism is the probable lack of extensively volatile-enriched mantle lithosphere capable of undergoing decompression melting west of 116°W. Old, volatile-enriched lithospheric mantle would not have been present west of this longitude because it presumably would have been stripped away by Late Cretaceous and early Tertiary shallow underthrusting of the Farallon plate (oceanic Pelona-Orocopia-Rand schists). This subschist dry mantle would have been well below its solidus and difficult to melt unless extensively metasomatically veined prior to volcanism. This problem might be circumvented if the period of early Tertiary subduction served to sufficiently devolatilize the slab and metasomatize the sub-Mojave mantle west of 116°W (Glazner, 1990) such that early Miocene extension could then trigger synextensional melting. This scenario seems unlikely given that subduction was shallow enough to completely remove the subcrustal mantle west of 116°W. The generally depleted geochemical signatures of the early Miocene basalts of the western Mojave also would seem to preclude this scenario.

What then could have triggered volcanism across the Mojave Desert after the long period of avolcanic shallow subduction?

An enigmatic relationship between volcanism and plate-boundary processes has long been suggested by the northward sweep of volcanism that follows the northward migration of the Mendocino Fracture Zone and Mendocino Triple Junction in the southern Great Basin, western Basin and Range, and parts of the California Coast Ranges (e.g., Glazner and Supplee, 1982; Johnson and O'Neil, 1984; Fox et al., 1985).

Miocene volcanism in the Coast Range volcanic provinces has been convincingly linked to overriding of East Pacific Rise segments by the North American plate during the early Miocene (e.g., Cole and Basu, 1995) and formation of slab windows or slab gaps (Dickinson and Snyder, 1979; Severinghaus and Atwater, 1990; Dickinson, 1997). The depleted-mantle source for the Coast Range basalts (Cole and Basu, 1995) is similar to that for Mojave basalts west of 116°W and suggests a possible link between early Miocene plate-boundary volcanism and early Miocene volcanism in the Mojave Desert. The north edge of this slab window coincided with the subducted Mendocino Fracture Zone. The plate age south of the Mendocino Fracture Zone was much younger than that to the north of the Mendocino Fracture Zone, so the coherency and thermal state of the slab and the eastern edge of the slab window were poorly defined (Dickinson and Snyder, 1979; Severinghaus and Atwater, 1990; Spencer, 1994; Dickinson, 1997).

In the context of the Mojave Desert, the main objections to early Miocene slab window magmatism are (1) the poor correspondence between the timing of Miocene volcanism in the Coast Ranges (26–22 Ma and 18–14 Ma) and the timing of voluminous volcanism in the Mojave Desert (ca. 22–18 Ma) and (2) the uncertainty in the thermal state of the slab south of the Mendocino Fracture Zone at Mojave Desert longitudes (Dickinson, 1997).

The timing problem may be artificial because Mojave Desert volcanism is part of the more protracted northward sweep and thus overlaps the discrete pulses of magmatism in the Coast Ranges. Discrete outbursts of volcanism in the Coast Ranges may have been related to transient upwelling in successive slab windows as rise segments arrived at the trench (Dickinson, 1997). However, if mantle upwelling in slab windows is a transient phenomenon, then the continuous northward migration of volcanism is more difficult to explain. If a slab window extended beneath the Mojave Desert, then perhaps northward-migrating volcanism was triggered by localized convective upwelling along the trailing edge of the Mendocino Fracture Zone (i.e., the "wake") as the subducted plate drifted northward (e.g., Liu and Zandt, 1996). This upwelling could have produced depleted-mantle basalts west of 116°W. Sudden impingement of hot asthenosphere on the lithosphere due to upwelling could also have triggered melting of readily fusible lithospheric mantle, giving rise to enriched basalts east of 116°W, although it is not clear why asthenospheric basalts would not also be erupted. In fact, Howard (1993) documented that the earliest pre-extension volcanic rocks in the Colorado River area were oceanic-island–like alkalic basalts, which are commonly associated with slab windows in other areas (Storey et al., 1989).

The uncertainty in the thermal state of the subducted slab south of the subducted Mendocino Fracture Zone, at Mojave Desert longitudes, is a problem for an interpretation of volcanism triggered by a migrating slab window edge, especially for early Miocene volcanism in the eastern Mojave Desert. However, models invoking homogeneous lithosphere thickening followed by convective thinning and extensional decompression melting of the enriched lithospheric mantle probably oversimplify the processes leading to volcanism and extension across the Mojave Desert and elsewhere in the southern Great Basin and Basin and Range (Axen et al., 1993; Spencer et al., 1995). Any model for early Miocene volcanism across the Mojave Desert must ultimately be able to account for the geochemical and isotopic characteristics of the volcanic rocks and must also be consistent with the pre-Tertiary geologic history of the region and the pre-Miocene crustal and mantle structure.

CONCLUSIONS

1. Sr_i and $\varepsilon_{Nd(t)}$ are well correlated with bulk composition and longitude for rocks from the western Mojave Desert to the Colorado River area. Pb isotopic composition is less well correlated with bulk composition but also shows regular longitudinal variations.

2. Correlated variation of isotopic composition with bulk composition is attributable to widespread crustal contamination of basalts with crustal materials.

3. Correlated variation in isotopic composition (Sr_i and $\varepsilon_{Nd(t)}$, whole-rock Pb, and previous quartz $\delta^{18}O$) with longitude reflects variations in mantle and crustal lithospheric structure from west to east across the Mojave Desert. Marked enrichments in LILEs and LREEs, low ratios of HFSEs to LILEs, and high Sr_i and low $\varepsilon_{Nd(t)}$ values in mafic rocks east of 116°W indicate a fairly abrupt change in mantle source east of this longitude when these rocks were erupted. Mantle east of 116°W was pre-Phanerozoic subcontinental lithospheric mantle, whereas mantle to the west of this longitude was depleted (suboceanic) mantle. The presence of subcontinental mantle lithosphere east of 116°W during Miocene volcanism also indicates that shallow subduction did not completely strip away the mantle lithosphere, in keeping with previous studies.

4. Isotopic characteristics of intermediate-composition and silicic rocks indicate that some minor percentage of thinned and probably reworked Precambrian crust probably extended farther west than 116°W along the sample transect. However, the data of this study and previous studies suggest that 116°W also marks a poorly understood crustal boundary. This boundary coincides with the southern projection of the Death Valley fault zone, a change in the dominant orientation of mountain ranges, the eastern limit of right-lateral faulting in the Mojave Desert, and the eastern limit of modern-day seismicity. The underthrust Pelona-Orocopia-Rand schists are inferred to extend to this boundary at depth in the crust; thus this longitude may approximately delineate a pronounced transition in overall lithospheric strength.

5. The problems surrounding the position of the $Sr_i = 0.706$ isopleth in the Mojave Desert and southern Sierra Nevada can be eliminated if the redefinition of the $Sr_i = 0.706$ line as an isopleth marking the western limit of pre-Phanerozoic North American mantle is adopted (Coleman and Glazner, 1997). By this definition, the $Sr_i = 0.706$ line would coincide with the isotopic break at 116°W in the Mojave Desert.

6. The outburst of early Miocene volcanism in the Mojave Desert cannot be explained exclusively by homogeneous crustal thickening followed by convective thinning, extension, and decompression melting of the lithospheric mantle, as has been previously proposed for rocks in the Colorado River area. Depleted-mantle basalts that erupted west of 116°W suggest a possible connection to coeval slab-window magmatism at the plate boundary, but the eastern limits of the slab window and the thermal state of the slab beneath the Mojave Desert in the early Miocene remain poorly known.

ACKNOWLEDGMENTS

Numerous scientists and colleagues working in the Mojave Desert and southeastern California have contributed to this project. We are especially indebted to Keith Howard, Jane Nielson, Dave Miller, and Joe Wooden of the U.S. Geological Survey in Menlo Park for helpful discussions, for logistical support, and for providing some samples. Drew Coleman, Rick Hazlett, Calvin Miller, Andy Sabin, Liz Schermer, and Doug Walker also provided assistance through helpful discussion, sample collection, laboratory assistance, and/or field assistance. Thanks are owed to Rick Carlson, Nick Rogers, and Clark Johnson for providing exceptional and thorough journal reviews. Support was provided by National Science Foundation grants EAR-8816941 and EAR-9204961 to Glazner, the Geochemical Trust Fund of the University of North Carolina Department of Geology, and a Martin Fellowship to Miller administered through the Department of Geology at the University of North Carolina. Miller also thanks the Department of Geology at San Jose State University for release time during revision of the manuscript.

REFERENCES CITED

Asmerom, Y., Jacobsen, S.B., and Wernicke, B.P., 1994, Variations in magma source regions during large-scale continental extension, Death Valley region, western United States: Earth and Planetary Science Letters, v. 125, p. 235–254.

Axen, G.J., Taylor, W.J., and Bartley, J.M., 1993, Space-time patterns and tectonic controls of Tertiary extension and magmatism in the Great Basin of the western United States: Geological Society of America Bulletin, v. 105, p. 56–76.

Bassett, A.M., and Kupfer, D.H., 1964, A geologic reconnaissance in the southeastern Mojave Desert, California: California Division of Mines and Geology Special Report 83, 43 p.

Beard, B.L., and Johnson, C.M., 1997, Hafnium isotope evidence for the origin of Cenozoic basaltic lavas from the southwestern United States: Journal of Geophysical Research, v. 102, p. 20149–20178.

Bennett, V.C., and DePaolo, D.J., 1987, Proterozoic crustal history of the western United States as determined by neodymium isotopic mapping: Geological Society of America Bulletin, v. 99, p. 674–685.

Boettcher, S.S., and Walker, J.D., 1993, Geologic evolution of Iron Mountain, central Mojave Desert, California: Tectonics, v. 12, p. 372–386.

Bradshaw, T.K., Hawkesworth, C.J., and Gallagher, K., 1993, Basaltic volcanism in the southern Basin and Range: No role for a mantle plume: Earth and Planetary Science Letters, v. 116, p. 45–62.

Carlson, R.W., and Hart, W.K., 1987, Crustal genesis on the Oregon plateau: Journal of Geophysical Research, v. 92, p. 6191–6206.

Carr, M.D., Harris, A.G., Poole, F.G., and Fleck, R.J., 1992, Stratigraphy and structure of outer continental margin rocks in Pilot Knob Valley, north-central Mojave Desert: U.S. Geological Survey Bulletin 2015, 33 p.

Cole, R.B., and Basu, A.R., 1995, Nd-Sr geochemistry and tectonics of ridge subduction and middle Cenozoic volcanism in western California: Geological Society of America Bulletin, v. 107, p. 167–179.

Coleman, D.S., Glazner, A.F., Miller, J.S., Bradford, K.J., Frost, T.P., Joye, J.L., and Bachl, C.A., 1995, Exposure of a Late Cretaceous layered mafic-felsic magma system in the central Sierra Nevada batholith, California: Contributions to Mineralogy and Petrology, v. 120, p. 129–136.

Coleman, D.S., and Glazner, A.F., 1997, The Sierra crest magmatic event: Rapid formation of Juvenile crust during the Late Cretaceous in California: International Geology Review, v. 39, p. 768–787.

Coleman, D.S., Frost, T.P., and Glazner, A.F., 1992, Evidence from the Lamarck Granodiorite for rapid Late Cretaceous crust formation in California: Science, v. 258, p. 1924–1926.

Cribb, J.W., and Barton, M., 1996, Geochemical effects of decoupled fractional crystallization and crustal assimilation: Lithos, v. 37, p. 293–307.

Daley, E.E., and DePaolo, D.J., 1992, Isotopic evidence for lithospheric thinning during extension: Southeastern Great Basin: Geology, v. 20, p. 104–108.

Darton, N.H., et al., 1915, Guidebook of the western United States: Part C. The Santa Fe route: U.S. Geological Survey Bulletin 613, 194 p.

Davis, G.A., 1977, Limitations on displacement and the southeastward extent of the Death Valley fault zone, California: California Division of Mines and Geology Special Report 129, p. 27–33.

Davis, J.M., and Hawkesworth, C.J., 1995, Geochemical and tectonic transitions in the evolution of the Mogollon-Datil Volcanic Field, New Mexico, U.S.A.: Chemical Geology, v. 119, p. 31–53.

Dickinson, W.R., 1997, Tectonic implications of Cenozoic volcanism in coastal California: Geological Society of America Bulletin, v. 109, p. 936–954.

Dickinson, W.R., and Snyder, W.S., 1979, Geometry of subducted slabs related to San Andreas transform: Journal of Geology, v. 87, p. 609–627.

Ducea, M.N., and Saleeby, J.B., 1998, The age and origin of a thick mafic-ultramafic keel beneath the Sierra Nevada batholith: Contributions to Mineralogy and Petrology, v. 133, p. 169–185.

Eugster, O., Tera, F., Burnett, D.S., and Wasserburg, G.J., 1970, The isotopic composition of gadolinium and neutron capture effects in some meteorites: Journal of Geophysical Research, v. 75, p. 2753–2768.

Faris, J.P., and Warton, J.W., 1962, Anion exchange resin separation of the rare earths, yttrium, and scandium in nitric acid–methnol mixtures: Analytical Chemistry, v. 34, p. 1077–1080.

Farmer, G.L., Perry, F.V., Semken, S., Crowe, B., Curtis, D., and DePaolo, D.J., 1989, Isotopic evidence of the structure and origin of subcontinental lithospheric mantle in southern Nevada: Journal of Geophysical Research, v. 94, p. 7885–7898.

Farmer, G.L., Glazner, A.F., Wilshire, H.G., Wooden, J.L., Pickthorn, W.J., and Katz, M., 1995, Origin of late Cenozoic basalts at the Cima volcanic field, Mojave Desert, California: Journal of Geophysical Research, v. 100, p. 8399–8415.

Feuerbach, D.L., Smith, E.I., Walker, J.D., and Tangeman, J.A., 1993, The role of the mantle during crustal extension: Constraints from geochemistry of volcanic rocks in the Lake Mead area, Nevada and Arizona: Geological Society of America Bulletin, v. 105, p. 1561–1575.

Fillmore, R.P., Walker, J.D., Bartley, J.M., and Glazner, A.F., 1994, Development of three genetically related basins associated with detachment-style faulting: Predicted characteristics and an example from the central Mojave Desert, California: Geology, v. 22, p. 1087–1090.
Fitton, J.G., James, D., and Leeman, W.P., 1991, Basic magmatism associated with Late Cenozoic extension in the western United States: Compositional variations in space and time: Journal of Geophysical Research, v. 96, p. 13693–13711.
Fox, K.F., Fleck, R.J., Curtis, G.H., and Meyer, C.E., 1985, Implications of the northwestwardly younger age of the volcanic rocks of west-central California: Geological Society of America Bulletin, v. 96, p. 647–654.
Gans, P.B., Mahood, G.A., and Schermer, E.R., 1989, Synextensional magmatism in the Basin and Range province: A case study from the eastern Great Basin: Geological Society of America Special Paper 233, 53 p.
Glazner, A.F., 1988, Stratigraphy, structure, and potassic alteration of Miocene volcanic rocks in the Sleeping Beauty area, central Mojave Desert, California: Geological Society for America Bulletin, v. 100, p. 424–435.
Glazner, A.F., 1990, Recycling of continental crust in Miocene volcanic rocks from the Mojave block, southern California: Geological Society of America Memoir 174, p. 147–168.
Glazner, A.F., and Bartley, J.M., 1984, Timing and tectonic setting of Tertiary low-angle normal faulting and associated magmatism in the southwestern United States: Tectonics, v. 3, p. 385–396.
Glazner, A.F., and O'Neil, J.R., 1989, Crustal structure of the Mojave Desert, California: Inferences from Sr and O isotope studies of Miocene volcanic rocks: Journal of Geophysical Research, v. 94, p. 7861–7870.
Glazner, A.F., and Supplee, J.A., 1982, Migration of Tertiary volcanism in the southwestern United States and subduction of the Mendocino Fracture Zone: Earth and Planetary Science Letters, v. 60, p. 429–436.
Glazner, A.F., Bartley, J.M., and Walker, J.D., 1989, Magnitude and significance of Miocene crustal extension in the central Mojave Desert, California: Geology, v. 17, p. 50–53.
Goter, S.K., Oppenheimer, D.H., Mori, J.J., Savage, M.K., and Masse, R.P., 1994, Earthquakes in California and Nevada: U.S. Geological Survey Open File Report 94–647, Map.
Hamilton, W.B., and Myers, W.B., 1966, Cenozoic tectonics of the western United States: Reviews of Geophysics, v. 4, p. 509–549.
Hanchar, J.M., Miller, C.F., Wooden, J.L., Bennett, V.C., and Staude, J-M.G., 1994, Evidence from xenoliths for a dynamic lower crust, eastern Mojave Desert, California: Journal of Petrology, v. 35, p. 1377–1415.
Hart, S.R., 1984, A large-scale isotope anomaly in the Southern Hemisphere mantle: Nature, v. 28, p. 753–757.
Hawkesworth, C., Turner, S., Gallagher, K., Hunter, A., Bradshaw, T., and Rogers, N., 1995, Calc-alkaline magmatism, lithospheric thinning, and extension in the Basin and Range: Journal of Geophysical Research, v. 100, p. 10271–10286.
Hazlett, R.W., 1986, Geology of a Tertiary volcanic center, Mopah Range, San Bernardino County, California [Ph.D. thesis]: Los Angeles, University of Southern California, 303 p.
Hildreth, W., and Moorbath, S., 1988, Crustal contributions to arc magmatism in the Andes of central Chile: Contributions to Mineralogy and Petrology, v. 98, p. 455–489.
Hileman, G.E., Miller, C.F., and Knoll, M.A., 1990, Mid-Tertiary structural evolution of the Old Woman Mountains area: Implications for crustal extension across southeastern California: Journal of Geophysical Research, v. 95, p. 581–614.
Houseman, G.A., McKenzie, D.P., and Molnar, P., 1981, Convective instability of a thickened boundary layer and its relevance for thermal evolution of continental convergence belts: Journal of Geophysical Research, v. 86, p. 6115–6132.
Howard, K.A., 1993, Volcanic history of the Colorado River extensional corridor: Active or passive rifting?: Geological Society of America Abstracts with Programs, v. 25, no. 5, p. 54.
Howard, K.A., and John, B.E., 1987, Crustal extension along a rooted system of imbricate low-angle faults: Colorado River extensional corridor, California and Arizona, *in* Coward, M.P., Dewey, J.F., and Hancock, P.L., Continental extensional tectonics: Geological Society [London] Special Publication 28, p. 299–311.
Howard, K.A., John, B.E., and Miller, C.F., 1987, Metamorphic core complexes, Mesozoic ductile thrusts, and Cenozoic detachments: Old Woman Mountains–Chemheuvi Mountains transect, California and Arizona, *in* Davis, G.H., and VandenDolder, E.M., eds., Geologic diversity of Arizona and its margins: Excursions to choice areas, field trip guidebook, Geological Society of America 100th Annual Meeting: Arizona Bureau of Geology and Mineral Technology Special Paper 5, p. 365–382.
Ingersoll, R.V., 1982, Triple-junction instability as cause for late Cenozoic extension and fragmentation of the southwestern United States: Geology, v. 10, p. 621–624.
Jacobson, C.E., Dawson, M.R., and Postlethwaite, C.E., 1988, Structure, metamorphism, and tectonic significance of the Pelona, Orocopia, and Rand schists, southern California, *in* Ernst, W.G., ed., Metamorphism and crustal evolution of the western United States (Rubey Volume VII): Englewood Cliffs, New Jersey, Prentice-Hall, p. 976–997.
Jennings, C.W., 1977, Geologic map of California: California Division of Mines and Geology, scale 1:750 000.
Johnson, C.M., and O'Neil, J.R., 1984, Triple junction magmatism: A geochemical study of Neogene volcanic rocks in western California: Earth and Planetary Science Letters, v. 71, p. 241–262.
Karlstrom, K.E., and Bowring, S.A., 1988, Early Proterozoic assembly of tectonostratigraphic terranes in southwestern North America: Journal of Geology, v. 96, p. 561–576.
Keith, L.A., Miller, J.S., Glazner, A.F., and Schermer, E.L., 1994, Geochemistry of Miocene volcanism on Fort Irwin, northern Mojave Desert, California: Geological Society of America Abstracts with Programs, v. 26, no. 2, p. 62–63.
Kistler, R.W., 1990, Two different lithosphere types in the Sierra Nevada, California, in Anderson, J.L., ed., The nature and origin of Cordilleran magmatism: Geological Society of America Memoir 174, p. 271–281.
Kistler, R.W., and Peterman, Z.E., 1973, Variations in Sr, Rb, K, Na, and initial $^{87}Sr/^{86}Sr$ in Mesozoic granitic rocks and intruded wall rocks in central California: Geological Society of America Bulletin, v. 84, p. 3489–3512.
Kistler, R.W., and Peterman, Z.E., 1978, Reconstruction of crustal blocks of California on the basis of initial strontium isotopic compositions of Mesozoic granitic rocks: U.S. Geological Survey Professional Paper 1071, 17 p.
Leeman, W.P., and Harry, D.L., 1993, A binary source model for extension-related magmatism in the Great Basin, western North America: Science, v. 262, p. 1550–1554.
Liu, M., and Zandt, G., 1996, Convective thermal instabilities in the wake of the migrating Mendocino triple junction, California: Geophysical Research Letters, v. 23, p. 1573–1576.
Livaccari, R.F., and Perry, F.V., 1993, Isotopic evidence for preservation of Cordilleran lithospheric mantle during the Sevier-Laramide orogeny, western United States: Geology, v. 21, p. 719–722.
Martin, M.W., and Walker, J.D., 1992, Extending the western North American Proterozoic and Paleozoic continental crust through the Mojave Desert: Geology, v. 20, p. 753–756.
Martin, M.W., Glazner, A.F., and Walker, J.D., 1993, Evidence for right-lateral transfer faulting accommodating en echelon Miocene extension, Mojave Desert, California: Geology, v. 21, p. 355–358.
Masi, U., O'Neil, J.R., and Kistler, R.W., 1981, Stable isotopes in Mesozoic granites of central and northern California and southwestern Oregon: Contributions to Mineralogy and Petrology, v. 76, p. 116–126.
Menzies, M.A., 1989, Cratonic, circumcratonic, and oceanic mantle domains beneath the western United States: Journal of Geophysical Research, v. 94, p. 7899–7915.
Miller, J.S., 1989, The Tertiary volcanic history and petrology of the Old Woman Mountains area, eastern Mojave Desert, California [M.S. thesis]: Nashville, Tennessee, Vanderbilt University, 160 p.
Miller, J.S., and Glazner, A.F., 1995, Jurassic plutonism and crustal evolution in the central Mojave Desert, California: Contributions to Mineralogy and Petrology, v. 118, p. 379–395.
Miller, J.S., and Glazner, A.F., 1997, Correlation of basalt sources with seismicity in California and western Nevada: Geological Society of America Abstracts with Programs, v. 29, no. 6, p. A-279.
Miller, J.S., and Miller, C.F., 1991, Tertiary extension-related volcanism, Old Woman Mountains area, eastern Mojave Desert, California: Journal of Geophysical Research, v. 96, p. 13629–13644.
Miller, C.F., and Wooden, J.L., 1994, Anatexis, hybridization and the modification of ancient crust: Mesozoic plutonism in the Old Woman Mountains area, California: Lithos, v. 32, p. 111–133.
Miller, J.S., Walker, J.D., Glazner, A.F., and Martin, M.W., 1995, Geochronologic and isotopic evidence for Triassic–Jurassic emplacement of the eugeoclinal allochthon in the Mojave Desert region, California: Geological Society of America Bulletin, v. 107, p. 1441–1457.
Miller, J.S., Glazner, A.F., and Crowe, D.E., 1996, Muscovite-garnet granites in the Mojave Desert: Relation to crustal structure of the Cretaceous arc: Geology, v. 24, p. 335–338.
Miller, J.S., Heizler, M.T., and Miller, C.F., 1998, Timing of magmatism, basin formation, and tilting at the west edge of the Colorado River extensional corridor: Results from single-crystal $^{40}Ar/^{39}Ar$ geochronology of Tertiary rocks in the Old Woman Mountains area, southeastern California: Journal of Geology, v. 106, p. 195–209.
Mukasa, S.B., and Wilshire, H.G., 1997, Isotopic and trace element compositions of upper mantle and lower crustal xenoliths, Cima volcanic field, California: Implications for evolution of the subcontinental lithospheric mantle: Journal of Geophysical Research, v. 102, p. 20133–20148.
Nielson, J.E., and Beratan, K.K., 1990, Tertiary basin development and tectonic implications, Whipple detachment system, Colorado River extensional corridor, California and Arizona: Journal of Geophysical Research, v. 95, p. 599–614.
Nielson, J.E., and Beratan, K.K., 1995, Stratigraphic and structural synthesis of a Miocene extensional terrane, southeast California and west-central Arizona: Geological Society of America Bulletin, v. 107, p. 241–252.
Nielson, J.E., Lux, D.R., Dalrymple, G.B., and Glazner, A.F., 1990, Age of the Peach Springs Tuff, southeastern California and western Arizona: Journal of Geophysical Research, v. 95, p. 571–580.
Parsons, T., and McCarthy, J., 1995, The active southwest margin of the Colorado Plateau: Uplift of mantle origin: Geological Society of America Bulletin, v. 107, p. 139–147.
Perry, F.V., Baldridge, W.S., and DePaolo, D.J., 1987, Role of asthenosphere and lithosphere in the genesis of late Cenozoic basaltic rocks from the Rio Grande Rift and adjacent areas of the southwestern United States: Journal of Geophysical Research, v. 92, p. 9193–9213.
Platt, J.P., and England, P.C., 1993, Convective removal of lithosphere beneath mountain belts: Thermal and mechanical consequences: American Journal of Science, v. 293, p. 307–336.
Reiners, P.W., Nelson, B.K., and Ghiorso, M.S., 1995, Assimilation of felsic crust by basaltic magma: Thermal limits and extent of crustal contamination of mantle-derived magmas: Geology, v. 23, p. 563–566.
Rogers, N.W., Hawkesworth, C.J., and Ormerod, D.S., 1995, Late Cenozoic basaltic magmatism in the western Great Basin, California and Nevada: Journal of Geophysical Research, v. 100, p. 10287–10301.
Sabin, A.E., Monastero, F.C., and Katzenstein, A.M., 1994, Middle to late Miocene age stratovolcano on the South Ranges, Naval Air Weapons Station, San Bernardino County, California, *in* McGill, S.F. and Ross, T.M., Geological investigations of an active margin: Geological Society of America Cordilleran Section Guidebook, San Bernardino Co. Museum Association, 2024 Orange Tree Lane, Redlands, California, p. 293–301.
Severinghaus, J., and Atwater, T., 1990, Cenozoic geometry and thermal state of the subducting slabs beneath western North America, *in* Wernicke, B.P., ed., Basin and Range extensional tectonics near the latitude of Las Vegas, Nevada: Geological Society of America Memoir 176, p. 1–22.
Sherrod, D.R., and Nielson, J.E., 1993, Tertiary stratigraphy of highly extended terranes, California, Arizona, and Nevada: U.S. Geological Survey Bulletin 2053, 250 p.
Sisson, T.W., Grove, T.L., and Coleman, D.S., 1996, Hornblende gabbro sill complex at Onion Valley, California, and a mixing origin for the Sierra Nevada batholith: Contributions to Mineralogy and Petrology, v. 126, p. 81–108.
Spencer, J.E., Richard, S.M., Reynolds, S.J., Miller, R.J., Shafiqullah, M., Gilbert, W.G., and Grubensky, M.J., 1995, Spatial and temporal relationship between mid-Tertiary

magmatism and extension in southwestern Arizona: Journal of Geophysical Research, v. 100, p. 10321–10351.

Stacey, J.S., and Kramers, J.D., 1975, Approximation of terrestrial lead isotope evolution by a two-stage model: Earth and Planetary Science Letters, v. 26, p. 207–221.

Stewart, J.H., and Poole, F.G., 1974, Lower Paleozoic and uppermost Precambrian Cordilleran miogeocline, Great Basin, western United States: Society of Economic Paleontologists and Mineralogists Special Publication 22, p. 28–57.

Stone, P., Howard, K.A., and Hamilton, W.B., 1983, Correlation of metamorphosed Paleozoic strata of the southeastern Mojave Desert region, California and Arizona: Geological Society of America Bulletin, v. 94, p. 1135–1147.

Storey, M., Rogers, G., Saunders, A.D., and Terrell, D.J., 1989, San Quentin volcanic field, Baja California, Mexico: "Within-plate" magmatism following ridge subduction: Terra Nova, v. 1, p. 195–202.

Suayah, I.B., Miller, J.S., Glazner, A.F., Martin, M.W., and Coleman, D.S., 1992, Mixing and assimilation in the Miocene Fremont Peak dike swarm, central Mojave Desert, California: EOS (Transactions, American Geophysical Union), v. 73, p. 659.

Sun, S-s., and McDonough, W.F., 1989, Chemical and isotopic systematics of oceanic basalts: Implications for mantle composition and processes, *in* Saunders, A.D., and Norry, M.J., eds., Magmatism in the ocean basins: Geological Society [London] Special Publication 42, p. 313–345.

Walker, J.D., and Coleman, D.S., 1991, Geochemical constraints on mode of extension in the Death Valley region: Geology, v. 19, p. 971–974.

Walker, J.D., Fletcher, J.M., Fillmore, R.P., Martin, M.W., Taylor, W.J., Glazner, A.F., and Bartley, J.M., 1995, Connection between igneous activity and extension in the central Mojave metamorphic core complex: Journal of Geophysical Research, v. 100, p. 10477–10494.

Wilshire, H.G., Meyer, C.E., Nakata, J.K., Calk, L.C., Shervais, J.W., Nielson, J.E., and Schwarzman, E.C., 1988, Mafic and ultramafic xenoliths from volcanic rocks of the western United States: U.S. Geological Survey Professional Paper 1443, 179 p.

Wilson, M., 1989, Igneous petrogenesis: London, Unwin Hyman, 466 p.

Wooden, J.L., and Miller, 1990, Chronologic and isotopic framework for Early Proterozoic crustal evolution in the eastern Mojave Desert region, SE California: Journal of Geophysical Research, v. 95, p. 20133–20146.

Wooden, J.L., Stacey, J.S., Howard, K.A., Doe, B.R., and Miller, D.M., 1988, Lead isotopic evidence for the formation of Proterozoic crust in the southwestern United States, *in* Ernst, W.G., ed., Metamorphism and crustal evolution of the western United States (Rubey Volume VII): Englewood Cliffs, New Jersey, Prentice-Hall, p. 69–86.

Young, E.D., Wooden, J.L., Shieh, Y-N., and Farber, D., 1992, Geochemical evolution of Jurassic diorites from the Bristol Lake region, California, USA, and the role of assimilation: Contributions to Mineralogy and Petrology, v. 10 p. 68–86.

Manuscript Received by the Society October 6, 1997
Revised Manuscript Received December 7, 1999
Manuscript Accepted December 9, 1999

Printed in USA